Review | Open Access

Catalysis, Energy and Environment

Hu et al. Catal. Energy Environ. 2026, 1, 6 DOI:10.20517/cee.2026.10

Expanding electrocatalytic nitrate and N_2 reduction beyond ammonia: N–N and S–N coupling toward value-added products

Yi Hu[1,2,#], Junxiao Wang[1,2,#], Zongyao Wang[1,2,#], Jiangyan Wang[1,2], Jiawei Wan[1,2,*], Dan Wang[3,*]

Keywords: Electrocatalysis, N–N coupling, S–N coupling, selectivity control, tandem catalysis, value-added nitrogen chemicals

Citation: Hu, Y.; Wang, J.; Wang, Z.; Wang, J.; Wan, J.; Wang, D. Expanding electrocatalytic nitrate and N_2 reduction beyond ammonia: N-N and S-N coupling toward value-added products. *Catal. Energy Environ.* **2026**, *1*, 6. https://dx.doi.org/10.20517/cee.2026.10

Received: 27 Jul 2026 **First Decision:** 18 Aug 2026 **Revised:** 24 Aug 2026 **Accepted:** 14 Sep 2026 **Published:** 28 Sep 2026

Academic Editor: Yongfa Zhu **Copy Editor:** Tong Wang **Production Editor:** Tong Wang

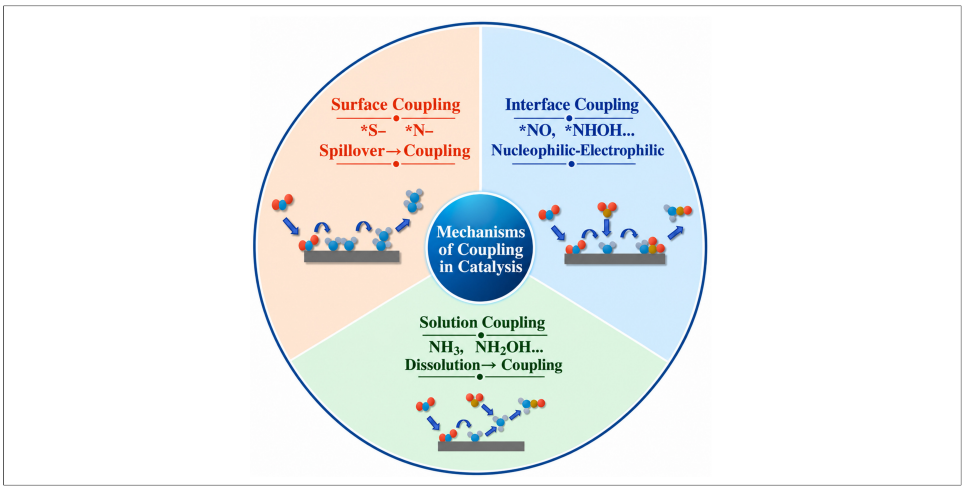

Abstract

Electrocatalytic reductions of nitrate (NO_3^-) and nitrogen (N_2) to ammonia (NH_3) have been extensively studied as a decentralized and sustainable alternative to the Haber-Bosch process. Recent studies have begun to move beyond ammonia synthesis toward the direct construction of value-added nitrogenous chemicals via N–N and S–N bond formation on electrocatalyst surfaces. This shift introduces catalyst-design requirements distinct from those for ammonia production: rather than maximizing $*NH_2$ hydrogenation and desorption, the catalyst must now accumulate surface $*NH_2$ intermediates, suppress over-hydrogenation, and enable selective coupling with a second nitrogen- or sulfur-containing species. This Review examines these challenges and the strategies proposed to address them. We begin by analyzing the key branch points within the NO_3^-/N_2 reduction network where the reaction can be kinetically intercepted to enable N–N coupling (to hydrazine and azo compounds) or S–N coupling (to sulfonamides and related motifs). We then survey

[1]State Key Laboratory of Biopharmaceutical Preparation and Delivery, Institute of Process Engineering, Chinese Academy of Sciences, Beijing 100190, China.
[2]School of Chemical Engineering, University of Chinese Academy of Sciences, Beijing 100049, China.
[3]College of Chemistry and Environment Engineering, Shenzhen University, Shenzhen 518060, Guangdong, China.
[#]These authors contributed equally to this work and share first authorship.

[*]**Correspondence to:** Prof. Jiawei Wan, State Key Laboratory of Biopharmaceutical Preparation and Delivery, Institute of Process Engineering, Chinese Academy of Sciences, Beijing 100190, China. E-mail: jwwan@ipe.ac.cn; Prof. Dan Wang, College of Chemistry and Environment Engineering, Shenzhen University, Shenzhen 518060, Guangdong, China. E-mail: danwang@szu.edu.cn

catalyst design strategies for each coupling pathway, including active site engineering for selective intermediate stabilization, dual-site synergy for co-adsorption of distinct coupling partners, and tandem catalyst configurations that physically separate $*NH_2$ generation from the subsequent coupling step. We critically evaluate design principles transferable from the more mature C–N coupling literature for their applicability to N–N and S–N systems. Finally, we identify practical entry points for experimental studies and summarize priorities for catalyst and reactor design.

INTRODUCTION

The electrocatalytic reduction of nitrate (NO_3^-) and nitrogen (N_2) to ammonia (NH_3) has advanced considerably, but most studies still focus on ammonia production and devote less attention to the use of surface-bound intermediates for N–N and S–N bond formation. Recent work has begun to explore an alternative objective: instead of driving hydrogenation to completion, the catalyst must accumulate partially reduced species (e.g., $*NH_2$), suppress over-hydrogenation, and enable their selective coupling with a second nitrogen- or sulfur-containing partner. Coupling reactions often require coordination between surface and solution pathways. This objective changes the reaction requirements: coupling reactions have an inherently "half-surface, half-solution" character, requiring not only surface activation but also interfacial transport and solution-phase bond formation. As shown in Figure 1, the rapid growth of this emerging direction is reflected in recent publication statistics retrieved from the literature database.

In this Review, we examine strategies for constructing N–N bonds (to hydrazine, azo compounds) and S–N bonds (to sulfonamides) from NO_3^- and N_2. We classify the pathways into three types according to the location of the key coupling step: Type I (surface), Type II (surface-solution interface), and Type III (solution-phase tandem). Using C–N coupling as a methodological comparison, we assess which design principles may transfer to N–N and S–N systems and compare the near- and long-term feasibility of the three pathway types. The aim is to clarify how nitrate-derived intermediates might be directed toward these products.

FROM AMMONIA PRODUCTION TO COUPLING: A CHALLENGE SPANNING MULTIPLE PHASES

Maturity and limitations of electrocatalytic NO_3^-/N_2 reduction to NH_3

Over the past decade, the electrocatalytic reduction of NO_3^- and N_2 to ammonia has developed rapidly. Strategies such as heteroatom doping, alloying, crystal facet engineering, and defect engineering have substantially improved the Faradaic efficiency (FE) and yield of ammonia[1-5]. However, most studies still treat ammonia as the sole target: the reaction network is optimized for progressive hydrogenation, and NH_3 desorption is regarded as the endpoint[6,7]. This "desorption-as-endpoint" model overlooks the potential for nitrogen-containing intermediates to undergo N–N and S–N coupling at surfaces and interfaces. The schematic in Figure 2 provides a preliminary visual overview of three conceptual coupling regimes; full formal definitions and comparative discussion are elaborated in Section "Coordinating surface and solution processes" below.

The motivation also extends beyond synthetic chemistry to the broader challenge of sustainable nitrogen management. In 2008, the U.S. National Academy of Engineering identified "managing the nitrogen cycle" as one of the 14 Grand Challenges for Engineering in the 21st century[8]. Human activities, exemplified by the Haber-Bosch process for ammonia synthesis, have doubled the global nitrogen fixation rate relative to pre-industrial levels, triggering cascading environmental problems such as an intensified greenhouse effect, widespread water eutrophication[9], and the expansion of dead zones. Extending the goal of electrocatalytic nitrogen reduction from exclusive NH_3 production to controllable N–N and S–N coupling may help shift the nitrogen economy from a "linear consumption" model toward a "circular utilization" model[9-11].

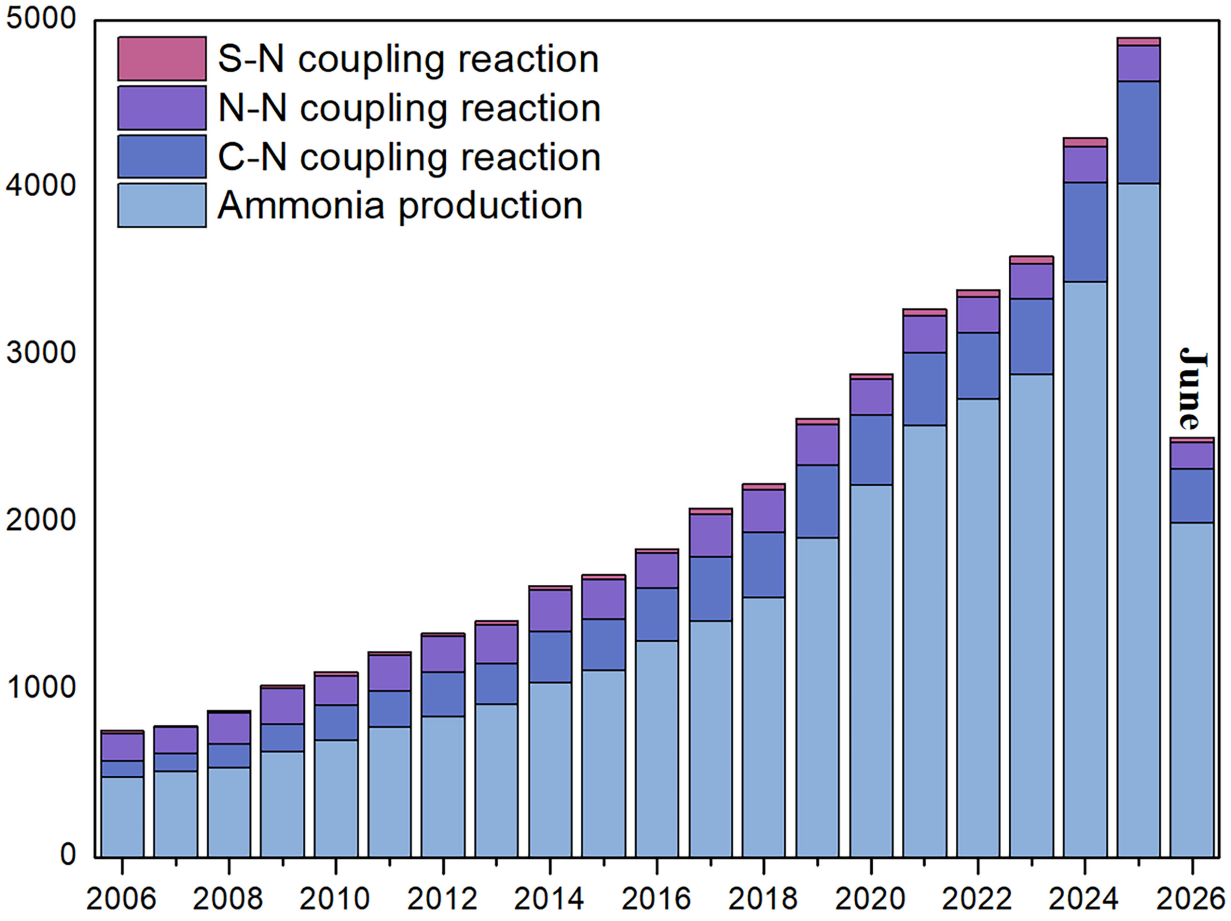

Figure 1. Recent publication volume from Web of Science (https://www.webofscience.com) on the synthesis of nitrogen-rich small molecules, including ammonia production and C–N, N–N, and S–N coupling reactions.

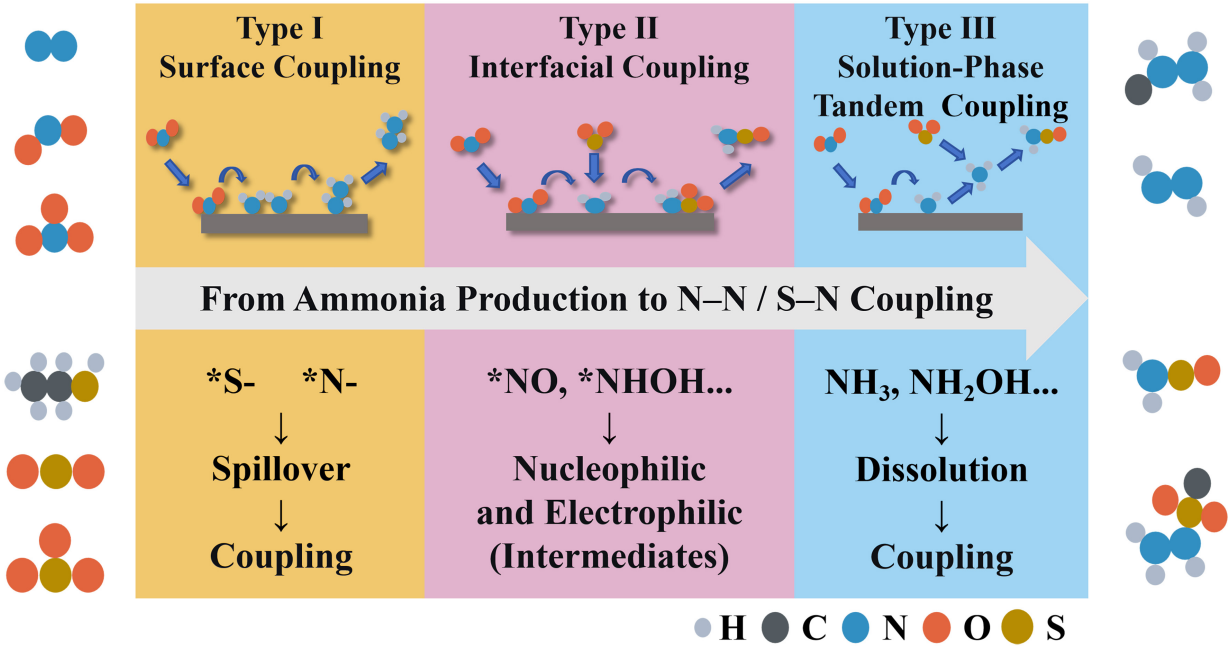

Figure 2. From ammonia production to selective N–N/S–N coupling via dual-region synergy. Schematic overview of three distinct electrocatalytic coupling regimes: Type I (Surface Coupling), Type II (Interfacial Coupling), and Type III (Solution-Phase Tandem Coupling).

Shifting the objective: from "desorption as the endpoint" to "desorption as the starting point"

The reaction strategy for ammonia production can be summarized as "intermediate → hydrogenation → desorption → product", in which all partially hydrogenated species are regarded merely as transient precursors on the pathway to NH_3[12-14].

When the target shifts to the construction of N–N or S–N bonds, the design objective changes: the reduction sequence need not proceed to completion; instead, the reduction state of reactive nitrogen species should be precisely controlled to prevent their complete conversion to ammonia. In this case, desorption no longer marks the reaction endpoint. Rather, the key design objective becomes controlling whether partially reduced nitrogen species are retained near the catalyst surface or transferred across the catalyst-electrolyte interface before subsequent bond formation. From a materials-design perspective, hierarchical hollow multi-shelled structures provide a potentially transferable platform for such spatial regulation. Their multiple shells and internal cavities can balance species confinement and transport, while heterointerfaces, defect engineering, and spatially ordered architectures can regulate interfacial stability and charge transfer[15-18]. Although these studies involve different electrochemical or photoelectric systems, these structural principles provide useful inspiration for controlling the surface-to-solution behavior of reactive intermediates. This revised strategy can therefore be expressed as "intermediate → hydrogenation suppression → desorption (or surface retention) → encounter with another molecule → bond formation"[19,20].

These steps can span multiple phases. In ammonia production, the key steps - adsorption, hydrogenation, deoxygenation, and product formation - occur almost exclusively on the solid surface, with the solution phase serving mainly as a medium for proton and electron supply and a reservoir for the final product[21]. In contrast, N–N and S–N coupling may exhibit a "half-surface, half-solution" character[21]: the adsorption and partial reduction of NO_3^- and the generation of active intermediates occur at the electrode surface, whereas these intermediates may desorb, diffuse, and ultimately form bonds in the interfacial electrical double layer or the bulk solution. Consequently, coupling catalysis cannot rely solely on the conventional surface-chemistry control strategy; it must simultaneously address selective partial reduction at the surface, species transport and lifetime matching at the interface, and the thermodynamic and kinetic conditions for bond formation in the solution phase.

C–N coupling, as the most mature electrocatalytic coupling system to date, serves as a useful methodological benchmark for N–N and S–N coupling. In 2026, Wu *et al.* reported a complete experimental workflow for electrocatalytic C–N bond construction in *Nature Protocols*[21], systematically covering catalyst synthesis, reactor construction, product quantification, and mechanistic characterization. This general design - activating a carbon source (CO_2, formic acid, aldehydes/ketones) to generate an electrophilic carbon intermediate, reducing a nitrogen source (NO_3^-/NO_2^-) to generate a nucleophilic nitrogen intermediate[21], and enabling their coupling on the electrode surface or in the near-interface region - parallels the "half-surface, half-solution" character outlined above. The catalyst design paradigm and operando characterization toolbox established in this work may inform the catalyst design and mechanistic investigation of N–N and S–N coupling[21].

Liu *et al.* demonstrated an ammonia-activation-mediated C–N coupling pathway, in which electrochemical oxidation of NH_3 generates active NH_2 species that subsequently couple with alcohol-derived species. By bypassing aldehyde formation and the associated overoxidation pathway, the system achieved a formamide productivity of 557.2 $\mu mol \cdot h^{-1} \cdot cm^{-2}$, a FE of 50.1%, and a carbon selectivity of 87.6%[22]. Together, these studies show that selectivity can be improved by changing the substrate activation sequence and coupling chronology, rather than solely by modifying catalyst composition. Beyond reaction-sequence control, dual-site cooperation can further facilitate C–N coupling through synergistic regulation of the band structure and

spin state[23].

Current status of C–N coupling (urea/amide synthesis)

Several catalyst-design strategies used in C–N coupling provide useful surface-reaction comparisons for the three pathways discussed here[24]. For example, in urea and amide synthesis via co-reduction of CO_2/CO and NO_3^-/NO_2^-, heteronuclear dual sites (e.g., Cu-Ce, Cu-Fe) offer separate active centers for CO reduction and nitrate reduction, respectively, promoting the coupling of surface *CO and *NH_2 by virtue of their spatial proximity[23,25]; single-atom catalysts (e.g., Fe-N-C, Cu-N-C) rely on coordination environment modulation to sequentially or synergistically activate both substrates at the same center[26]; oxygen-vacancy engineering on TiO_{2-x}[27] and CeO_{2-x}[28] exploits defect sites to shorten the adsorption distance between *CO and nitrogen-containing intermediates and lower the coupling barrier. These strategies predominantly follow the core strategy of the surface-localized regime, that is, achieving co-adsorption and lateral bond formation on the electrode surface. Representative electrocatalytic C–N bond formation examples, including urea, formamide, oxime, and amino‑acid electrosynthesis, have been well summarized in reference[21]. Three general design principles follow: (i) bi-component co-adsorption requires the two active sites to be intimately coupled at the nanoscale, with heteronuclear diatomic pairs or adjacent lattice sites being likely to be more effective than physical mixtures; (ii) the surface coverages of each species must be precisely balanced via potential and current density modulation, avoiding overaccumulation of either species that would favor competitive side reactions such as hydrogen evolution or deep reduction; and (iii) spatial separation of sites with different hydrogen affinities: for example, separating hydrogen evolution sites from nitrogen activation sites can effectively suppress the hydrogenation of NH_2, thereby promoting C–N bond formation.

Transferable principles from C–N to N–N/S–N coupling

When applying these principles to N–N and S–N coupling, one must clearly recognize their fundamental limitations: the success of C–N coupling relies heavily on the Type I strategy, benefiting from the fact that CO_2 and NO_3^- can be reduced/activated simultaneously on spatially separated yet intimately coupled dual sites without severe mutual interference or competitive poisoning. When applied to N–N coupling, this strategy is constrained by the ceiling of NH_2 surface coverage. When applied to S–N coupling, it is constrained by the irreversible chemisorption of sulfur species and the resulting poisoning of most metal surfaces. Therefore, breakthroughs in N–N and S–N coupling may require greater reliance on Type II (interfacial) and Type III (solution-phase tandem) strategies than is the case for C–N coupling, either by partitioning the intermediate species across the surface and solution via the interfacial region, or by fully decoupling the process into two stages: “electrochemical generation of specific intermediates and solution-phase chemical bond formation”. This comparison suggests a practical criterion: Type I is preferable when co-adsorption is feasible without severe interference; Type II or III may offer more control when coverage mismatch, poisoning, or incompatible reaction conditions dominate.

C–N coupling studies also show that catalyst performance depends on the wider reaction system. Liu systematically demonstrated four strategies - coordination anchoring, interface engineering, size reduction, and heterojunction construction - using Mo-based materials (MoS_2, MoB_2, and Mo single atoms) as platforms[29], all of which are relevant to surface and interfacial control. In addition, catalyst design should be considered together with reactor engineering, solution chemistry, and mass transfer.

Strategies for electrochemically constructing N–N and S–N bonds using NO_3^-/N_2 as the nitrogen source

This Review examines strategies and design principles for electrochemically constructing N–N and S–N bonds with NO_3^- and N_2 as nitrogen sources. We focus on two classes of products: N–N coupling products (hydrazine, azo compounds) and S–N coupling products (sulfonamides)[30,31]. With these two targets in mind

and drawing on the established experience of C–N coupling reactions, we categorize the coupling pathways into three fundamental modes: (i) surface direct coupling, which relies on lateral coupling of adsorbed nitrogen-containing intermediates (*NH_2, *NHOH, *NO, *etc.*) at high surface coverage; the competition between surface diffusion and hydrogenation/desorption is governed by the spatial proximity of active sites, control of adsorbate coverage, and suppression of hydrogen evolution[32,33]; (ii) interfacial coupling, in which partially hydrogenated species are allowed to desorb into the electrical double layer or the near-surface solution region and subsequently form bonds with dissolved co-reactants (SO_3^{2-}, thiols, *etc.*) near the surface; this pathway is highly sensitive to interfacial pH, electric field strength, residence time, and species lifetime matching[34,35]; and (iii) tandem chemical coupling, which decouples electrocatalytic and subsequent chemical steps in time and space by electrochemically generating relatively stable active intermediates (hydroxylamine, nitroso compounds, diazonium salts, *etc.*) *in situ*, which then undergo homogeneous or interface-assisted bond formation with another substrate in the solution phase[36-39]. The comparison is used to identify where each pathway may be practical and which limitations require experimental testing.

A TWO-ZONE MODEL OF THE REACTION: SYNERGY AND COMPETITION BETWEEN THE SURFACE AND THE SOLUTION

Generation, adsorption, and desorption of nitrogen-containing intermediates

Understanding how N–N and S–N coupling occurs in a heterogeneous environment first requires clarification of the range of nitrogen-containing intermediates within the NO_3^-/N_2 electroreduction network and their partitioning behavior. Through stepwise deoxygenation and hydrogenation, NO_3^- yields a sequence of species including NO_2^-, NO, NHOH, NH_2OH, NH_2, and NH_3[40,41]. The distribution of these species between the surface and the solution is governed by the interplay of four factors: (1) the binding energy between the intermediate and the surface: strongly chemisorbed species (e.g., NO adsorbed on Pt[42], Rh[43], and Cu[44]; *NH_2 forming M–N bonds on most transition metals) tend to remain surface-bound[45,46]; (2) the electrode potential, which not only drives the depth of reduction but also modulates adsorption strength through surface charge and electric field effects[47]; (3) local pH: protonation of NH_2OH and NH_3 in an acidic electrical double layer alters their charge and adsorption behavior[48,49]; and (4) water solubility: NH_2OH and NH_3, being highly water-soluble, readily escape into the solution and are difficult to return to the surface, whereas NO, with its limited solubility, tends to linger in the near-surface region[50].

Together, these factors define a kinetic boundary: strongly adsorbed species (such as NO and *NH_2) tend to remain on catalytic sites, whereas more weakly adsorbed species (such as NH_2OH and NH_3) are more likely to desorb into the interfacial region or bulk solution[45]. This demarcation is not absolute but is dynamically modulated by mass transport rates, adsorbate coverage, and competing reactions. This partitioning helps determine whether subsequent coupling can occur on the surface or after desorption.

Surface reaction zone: available tools and limitations

Strongly adsorbed surface-bound intermediates with high adsorption energies (NO, NH_2) can, in principle, undergo direct lateral coupling on the electrode surface. Possible control strategies include tuning the electronic structure of active sites to optimize intermediate adsorption energies and thereby lower the coupling activation barrier[51]; constructing dual-site synergistic arrays to promote bonding via spatial proximity[52]; and introducing confined microenvironments to prolong the surface lifetime of intermediates and restrict their orientation[53]. However, the surface reaction zone faces two main constraints. First, surface coverage depends strongly on the electrode potential and competitive adsorption equilibria; within the potential window driving reduction, the competition among protons, solvent molecules, and nitrogen-containing intermediates for active sites makes it difficult to independently control the coverage of each species[54]. Second, because protons persist, deep hydrogenation to NH_3 remains a strong competing pathway,

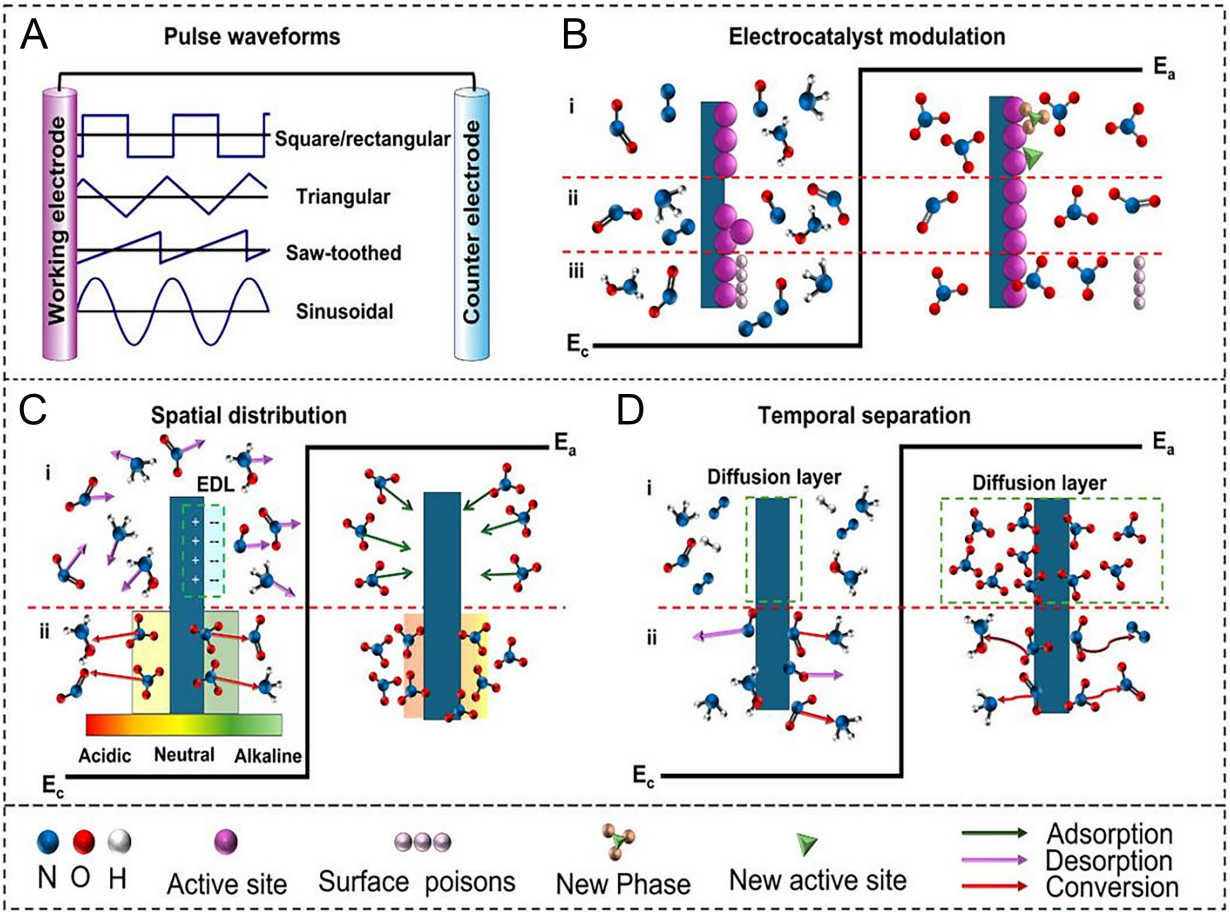

Figure 3. A schematic representation of (A) various pulse shapes, (B) electrocatalyst modulation, (C) spatial distribution, and (D) temporal separation. Reprinted with permission from reference[56] under the CC BY 4.0 license. EDL: Electrical double layer.

and the "retention" state of intermediates required for coupling can be easily disrupted. These two constraints mean that suppressing hydrogen evolution and over-hydrogenation solely through surface engineering is inherently challenging[55]. To address these limitations, pulsed electrolysis - a dynamic potential-modulation strategy - has emerged as a promising approach to overcoming the bottlenecks of steady-state electrolysis. Torabi *et al.* have systematically reviewed progress in pulsed electrolysis for the reduction of nitrogenous species, highlighting that periodic alternation between anodic and cathodic potentials enables dynamic surface restructuring of the catalyst, spatiotemporal modulation of the electrical double layer structure and interfacial pH, enhanced mass transport, and temporal separation of intermediates[56], which may help separate intermediate generation and coupling in time, as illustrated in Figure 3.

For N–N and S–N coupling, pulsed electrolysis follows three key design principles. First, temporal decoupling: alternating potentials separate the step of generating reactive nitrogen intermediates from subsequent coupling events, avoiding immediate over-hydrogenation to NH_3 under constant cathodic bias. Second, dynamic surface regeneration: short oxidative or open-circuit intervals intermittently strip adsorbed poisons (especially sulfur-containing species for S–N coupling) that would otherwise accumulate under steady reduction. Third, interfacial microenvironment tuning dynamically adjusts local pH, adsorbate coverage, and double-layer structure to maintain favorable conditions for bond formation, which cannot be sustained at fixed potentials.

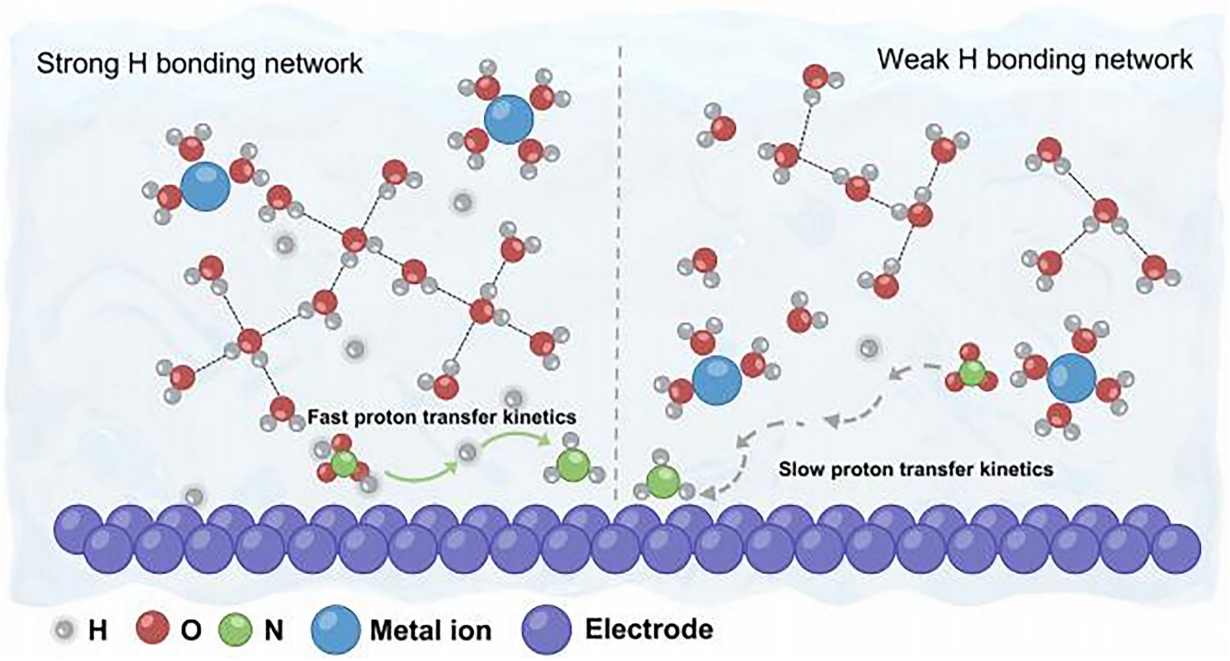

Figure 4. Representative H-bond networks at the water interface. Schematic depiction of enhanced H-bond connectivity facilitating nitrate reduction to ammonia. This schematic illustrates general interfacial hydrogen-bond network principles. Reprinted with permission from reference[63]. Copyright 2026 Wiley-VCH GmbH.

Concrete experimental evidence demonstrates its advantages over steady-state electrolysis. In nitrite electroreduction toward azo compounds, square-wave pulsed potential modulation achieved 42% FE for azo products, while the same catalyst under a constant reductive potential achieved only 17% FE for azo products. Periodic pulse refreshment reduced excess adsorbed hydrogen coverage and temporally matched the lifetime of short-lived nitrogen intermediates for interfacial N–N coupling. For reactions involving sulfur, which are highly relevant to prospective S–N coupling, pulsed electrolysis combining a reductive working potential with mild oxidative cleaning pulses greatly alleviated irreversible sulfur-poisoning of metallic electrodes. Relative to steady-state electrolysis, pulsed operation exhibited ~3.8-fold higher product selectivity over prolonged operation by preventing continuous sulfur site-blocking, offering important guidance for future S–N coupling investigations[57].

Solution reaction zone: overlooked degrees of freedom

In contrast to surface-bound species, which are subject to *H competition and coverage constraints, species that escape into the solution (NH_2OH, NH_3) introduce additional variables that can be controlled[58]. These include solvent selection (aqueous, organic, or mixed solvents) to modulate the solvation state and stability of intermediates[59]; precise pH control to alter the protonation state and nucleophilicity/electrophilicity of species[60]; the addition of redox mediators or chemical trapping agents to extend the effective lifetime of short-lived intermediates[61]; and the introduction of homogeneous catalysts to decouple the bond formation step from surface electron transfer[62].

Recently, electrolyte anion selection has also been exploited to modulate the solution microenvironment. Yang *et al.* discovered that CO_3^{2-} can repel interfacial hydrated K^+ ions, reduce the fraction of $K^+ \cdot H_2O$, and increase the proportion of four-coordinated hydrogen-bonded water, thereby enhancing proton conductivity by a factor of 317 and delivering an ammonia production rate of 76.36 $mg \cdot h^{-1} \cdot mg_{cat.}^{-1}$ with nearly 100% FE at -1.1 V *vs.* RHE. This result suggests that supporting anions can modify the reaction microenvironment by changing the interfacial water structure[63]. More generally, as illustrated in Figure 4, interfacial hydrogen-bond network regulation provides a general strategy for tuning proton transport and the reaction microenvironment.

The main advantage of the solution zone is that it provides multiple regulatory dimensions, including solvent, pH, mediators, and anion type, which allow greater control over substrate concentrations and ratios than is possible on a crowded surface[64]. However, key intermediates (imines, free hydrazine, hydroxylamine derivatives) can undergo hydrolysis or disproportionation in water and may have short lifetimes; under homogeneous conditions, selectivity control still requires system-specific optimization. This underscores the critical role of the interfacial "surface-to-solution" transition region in bridging surface generation and solution-phase bond formation.

Coordinating surface and solution processes

As discussed above, the catalyst surface, while offering the advantages of precise activation and confined microenvironment modulation, is constrained by the strong coupling between *H competition and intermediate coverage; the solution phase, while providing freedom in substrate ratios and synthetic strategies, is limited by the deactivation of short-lived intermediates and the lack of a general design methodology. Neither zone alone is optimal for every N–N or S–N coupling system. The design challenge is to match active-species generation at the surface with transport and bond formation in solution.

Confined water provides one physicochemical perspective on surface-solution coupling. Wang *et al.* have noted that water confined in nanocavities, on solid surfaces, in porous materials, or within high-concentration ionic layers exhibits enthalpic, entropic, and dielectric properties that deviate significantly from those of bulk water. For example, confinement can drastically reduce the static dielectric constant of water; the out-of-plane dielectric constant in hexagonal boron nitride nanochannels drops to ~2.1, only one-fortieth that of bulk water (~80), directly influencing the solvent reorganization energy and interfacial electron transfer rate in Marcus theory[65].

Building on the preliminary schematic overview shown in Figure 2, we now provide full formal definitions for the three distinct coupling regimes. We therefore classify coupling reactions into three types according to the location of the key bond-forming step: (i) the surface-localized regime. Two strongly adsorbed nitrogen-containing intermediates (e.g., *NH_2, *NO, *NHOH) meet directly on the electrode surface via lateral diffusion and couple. The entire bond-forming step occurs on the surface; this regime typically targets hydrazine and surface-anchored azo species[66]; (ii) the interfacial regime. An adsorbed intermediate generated on the surface (e.g., *NH_2, *NO) encounters and bonds with a solution-borne species (e.g., SO_3^{2-}, thiols, sulfinates) within the electrical double layer or the near-surface transition region. Such an interfacial configuration is proposed here as a potentially useful framework for S–N bond construction, with established electrochemical S–N bond formation involving SO_2 and amines providing a relevant methodological precedent[67]; (iii) The solution-phase tandem regime. The electrode serves merely as a generator of sufficiently stable intermediates that can readily escape into the solution (e.g., hydroxylamine, diazonium salts, nitroso compounds); once released into the bulk solution, these species undergo bond formation with another homogeneous partner, entirely decoupled from the electrode surface. The surface is responsible only for precursor generation. Typical examples include condensation or nucleophilic substitution coupling of hydroxylamine in solution to form oximes and organic amines[68].

This classification, using the spatial location of the coupling event as the criterion, bridges mature catalyst electronic structure design with the strategy of organic synthesis in solution, covering surface engineering, interfacial control, and homogeneous chemistry. As we move from the surface scenario to the interfacial scenario and finally to the solution-phase scenario, the degree of direct surface involvement in bond formation decreases, while the degrees of freedom afforded by solution-phase chemistry increase; concurrently, the requirements for intermediate stabilization and cross-region transport increase. The confinement effect, hydrogen-bonding network, and dielectric response of interfacial water are precisely the

key physicochemical variables that link the surface and the solution and regulate the cross-region behavior of species along this progression. In the subsequent sections of this Review, Sections "N–N COUPLING STRATEGIES: FROM SURFACE TO SOLUTION" and "S–N COUPLING: THEORETICAL FEASIBILITY AND CATALYST DESIGN PERSPECTIVES" are organized according to these three pathway types, dissecting the key principles of catalyst design, interfacial environment modulation, and cross-region synergy for each type, thereby illustrating the design strategy that leads from electrocatalytic hydrogenation/deoxygenation to selective redox coupling.

The boundary between the interfacial near-electrode region and the bulk electrolyte is continuous rather than atomically sharp. Accordingly, the Type II (interfacial) and Type III (solution-phase tandem) categories serve as conceptual working frameworks, and mixed contributions from both channels are frequently observed in practical experiments. Several experimental diagnostic criteria can help distinguish the dominant contribution of each pathway: (i) Mass-transport perturbation tests, in which stirring speed or electrolyte flow rate is varied. Strong flow-rate dependence of coupling selectivity suggests Type II interfacial coupling, where bond formation occurs within the near-surface diffusion layer; nearly flow-insensitive selectivity points toward Type III coupling occurring in the bulk solution; (ii) Rotating ring-disk electrode (RRDE) measurements, which quantify the fraction of electrogenerated intermediates escaping from the electrode surface. When coupling products form before intermediates fully depart the near-surface zone, Type II dominates; substantial intermediate collection on the ring electrode followed by downstream coupling supports Type III character; (iii) *In situ* interfacial vibrational spectroscopy, including attenuated total reflectance Fourier-transform infrared (ATR-FTIR) spectroscopy and surface-enhanced Raman spectroscopy (SERS). Detecting coupling-product fingerprints via surface-enhanced signals indicates interfacial Type II processes; the absence of surface-confined product signals with detection of products in bulk-solution samples favors Type III; (iv) Membrane-separated compartment electrolysis. Detecting coupled products in a post-electrolysis chemical reservoir without direct electrode contact strongly confirms Type III solution-phase coupling; negligible product formation in the downstream reservoir implies coupling is confined to the electrode-interfacial zone (Type II). In many practical systems, these tests reveal co-existing Type II and Type III contributions, and the classification merely identifies the kinetically dominant channel[69].

It is instructive to explicitly compare pathway preferences across C–N, N–N, and S–N coupling systems. Most well-developed C–N coupling examples, such as urea electrosynthesis, favor the Type I surface-coupling regime: CO_2-derived carbon intermediates and nitrate-derived nitrogen intermediates can be co-adsorbed on adjacent active sites without severe site blocking or poisoning, enabling lateral surface bond formation. In contrast, N–N coupling faces an intrinsic surface-coverage ceiling for key nitrogen intermediates (*NH_2, *NHOH), making pure Type I surface coupling difficult to sustain. Accordingly, N–N coupling more often follows Type II interfacial or Type III solution-tandem routes. For S–N coupling, the additional risk of irreversible chemisorption of sulfur species and catalyst poisoning further disfavors Type I surface co-adsorption. As a result, S–N coupling relies even more heavily upon Type II interfacial and Type III solution-phase tandem strategies, where bond-forming events are partially or fully decoupled from the catalyst surface[21,24].

N–N COUPLING STRATEGIES: FROM SURFACE TO SOLUTION

Practical significance of target products

Hydrazine (N_2H_4) is a key component of rocket propellants and a promising liquid hydrogen carrier. Azo and azoxy compounds serve not only as traditional chromophores for bulk dyes but also find unique applications in photoswitches and controlled-release prodrugs[70]. More notably, five-membered N–N-containing heterocycles, such as pyrazoles and 1,2,3-triazoles, have been explored as amide-bond bioisosteres in medicinal chemistry, where they can mimic key structural and electronic features of amides and provide

opportunities to modulate pharmacokinetic properties[71]. These applications motivate continued development of selective N–N synthesis.

Type I: surface N–N coupling from N_2 and NO_3^-

Conventional electrocatalytic N_2 reduction predominantly targets NH_3 through successive proton-coupled electron-transfer steps. In contrast, selective N_2-to-N_2H_4 conversion requires preservation of the N–N framework while terminating the reduction before complete hydrogenation to NH_3. Saha *et al.* demonstrated this possibility using a trinuclear T-shaped nickel thiolate molecular complex, whose electrochemically generated Ni(I) state reduced N_2 to N_2H_4 in the presence of PhOH as a proton donor, with hydrazine being the only detected nitrogen-containing product[72]. Although this molecular system is not itself a heterogeneous surface-coupling example, it establishes the electrochemical feasibility of selectively reducing N_2 to N_2H_4 while retaining the N–N bond. Translating such selectivity to heterogeneous aqueous electrocatalysis, however, remains highly challenging. This route faces two major bottlenecks. First, the extremely low aqueous solubility of N_2 severely limits mass transport, thereby restricting surface coverage and coupling rates[73]. Second, $*N_2H_x$ intermediates are inherently unstable under the sustained proton/electron flux at cathodic potentials, as the energy barriers separating N–N bond retention from over-hydrogenation or cleavage are vanishingly small; the intermediates readily undergo N–N bond cleavage to form $*NH_x$ or become fully hydrogenated and desorb as NH_3, making selective hydrazine production difficult[74].

In contrast to the N_2 route, which is constrained by poor solubility, NO_3^- offers aqueous concentrations up to several molar[73], substantially alleviating mass-transport limitations for surface-bound nitrogen intermediates. Along the stepwise deoxygenation/hydrogenation pathway of NO_3^-, $*NH_2$ is a possible building block for N–N bond construction, as lateral coupling of two $*NH_2$ species generates hydrazine[75]. However, this surface self-coupling of $*NH_2$ faces a challenge: hydrazine formation requires two adjacent $*NH_2$ species to encounter each other both spatially and temporally, a coverage threshold that is difficult to achieve on most metal surfaces because the competing hydrogenation of $*NH_2$ to NH_3 is thermodynamically accessible and the ubiquitous presence of adsorbed H (and its competition for active sites) readily quenches $*NH_2$ to NH_3[76].

In view of these challenges, most current studies targeting hydrazine have instead focused on the oxidative coupling of ammonia, rather than direct reduction of nitrogen oxides to hydrazine. A handful of exploratory nitrate electroreduction studies have detected only trace amount of hydrazine as a minor side-product, with ammonia as the overwhelmingly dominant product. For example, Cu_2O@COF and copper phthalocyanine-based catalytic systems produce only trace or microgram-scale amounts of hydrazine with extremely low FE. In practice, direct NO_x-to-hydrazine electroreduction suffers from multiple intrinsic bottlenecks: adsorbed nitrogen intermediates are kinetically driven toward deep hydrogenation to NH_3; any hydrazine that forms is vulnerable to further electrochemical degradation under cathodic conditions; and uncontrolled N–N coupling preferentially produces dinitrogen instead of hydrazine. These drawbacks prevent high-yield hydrazine synthesis through this direct pathway[77-78].

Type II: surface-solution interfacial coupling - insights from catalyst-solvent synergistic modulation in electrocatalytic coupling of nitroarenes

An interfacial route would require precise control of the oxidation state of surface intermediates together with stabilization and transport of solution-phase species. The surface task focuses on precisely arresting the nitrogen intermediate at a specific oxidation state: for azo synthesis starting from NO_3^-, the ideal interfacial active species are electrophilic NO_2^- or NO adducts, rather than the deeply reduced NH_2. This requires the catalyst to thermodynamically enhance the FE for the $NO_3^- \rightarrow NO_2^-$/NO pathway while kinetically

suppressing subsequent hydrogenation and deoxygenation steps[79].

Zhou *et al.* revealed the decisive role of Cu facet orientation in determining nitrate reduction selectivity[80]. Oxide-derived Cu cubes enriched with Cu(100) facets achieved an NH_3 FE of 93.9% and a yield rate of 219.8 μmol h^{-1}·cm^{-2} at -0.9 V *vs.* RHE, significantly outperforming Cu microspheres enriched with Cu(111) facets (81.7% FE). Density functional theory (DFT) calculations demonstrated that NO_3^- adsorption on Cu(100) is spontaneous (ΔG = -0.11 eV), with the rate-determining step being NH_3 desorption (barrier: 0.34 eV). In contrast, NO_3^- adsorption at the Cu/Cu_2O interface is endothermic (ΔG = +1.33 eV)[80], with the rate-determining step being the hydrogenation of NO to *NOH (barrier: 0.84 eV), explaining why the Cu^0 phase favors NH_3 formation while the Cu^+ phase stalls at the NO_2^- stage. *In situ* ATR-FTIR captured signals of -NH_2 (1,450 cm^{-1}) and NO_2^- (1,250 cm^{-1}) intermediates. These results show that facet engineering can modulate intermediate adsorption and hydrogenation barriers, thereby directing the reaction toward coupling rather than over-hydrogenation[80].

Cu-based materials, owing to their intrinsic high activity for NO_3^- reduction and weak hydrogen adsorption, are advantageous surfaces for generating and accumulating NO_2^-. Further alloying (e.g., Cu-Ni, Cu-Zn) or facet regulation can moderate the adsorption strength of key intermediates such as NO, preventing them from either binding too strongly (leading to deep hydrogenation) or too weakly (leading to complete desorption and escape), thereby maintaining a high-chemical-potential "nitroso pool" in the near-surface region[81,82]. In recent years, Fe-N-C single-atom sites have also demonstrated the ability to selectively generate *NH_2, with their coordination environment suppressing over-hydrogenation, offering the possibility of nucleophilic nitrogen building blocks for interfacial coupling that complement electrophilic NO_2^-/NO[83].

The solution-side task focuses on maintaining sufficient availability of aromatic amine coupling partners and promoting their interaction within the near-electrode region. Surface functionalization provides an effective strategy for regulating such interfacial interactions. For example, Qiao *et al.* demonstrated that surface hydroxyl groups on Ni_3Fe-MOF-OH enhance the adsorption of anilines and suppress competing electrochemical reactions, thereby promoting selective N–N coupling toward azo compounds[84]. Such control over substrate adsorption and interfacial reactivity provides a useful methodological precedent for matching aromatic amine coupling partners with surface-generated nitrogen intermediates in prospective Type II pathways.

However, the spatiotemporal matching between the surface and the solution remains a major challenge: once generated, NO_2^- is highly prone to disproportionation or protonation to evolve NO gas in acidic media, whereas the nucleophilic attack of aromatic amines requires a finite contact time. This demands that catalyst design for oxidation state control be coupled with interfacial microenvironment engineering, for instance, pulsed potential techniques that intermittently generate NO_2^- in synchronization with the refresh rate of the aromatic-amine diffusion layer, allowing interfacial coupling to outcompete unproductive side reactions and intermediate loss. This synergistic modulation framework provides a design blueprint for the direct electrosynthesis of azo pharmaceutical intermediates from NO_3^- and aromatic amines, while also laying a methodological foundation for subsequent S–N interfacial coupling (sulfonamides).

Type III: solution-phase N–N coupling (electrochemical-chemical tandem)

The Type III strategy fully separates precursor generation from bond formation: the electrode surface is used as a source of intermediates by efficiently generating nitrogen-containing species with sufficient chemical stability, such as NH_3 or NH_2OH, and releasing them into the bulk solution. The subsequent N–N coupling is then accomplished by an independent chemical catalytic step, entirely removed from the direct control of the

electrode surface and electric field[85]. The freedom afforded by this separation is twofold: the electrochemical module can focus on a single objective, maximizing the yield and FE of a specific intermediate (e.g., NH_2OH) without the competing effects of *H adsorption or over-hydrogenation; the chemical coupling module, in turn, can freely draw upon mature strategies from homogeneous catalysis, organic synthesis, and even enzymatic catalysis, independently optimizing temperature, solvent, catalyst ligands, and stoichiometric ratios[86]. From the perspective of surface reactions, both NH_2OH and NH_3 lie beyond the aforementioned dividing line and possess sufficiently long solution-phase lifetimes to allow flexible spatiotemporal control of the two steps. Typical configurations include directly feeding the electrolytic effluent into a downstream reactor or performing the tandem sequence in a one-pot system via sequential reagent addition. This design strategy not only liberates coupling selectivity from the constraints of surface potential but also allows the use of highly selective chemical coupling systems and may avoid some limitations of surface-mediated N–N bond formation.

The NH_4NO_3 liquid nitrogen fertilizer production system reported by Han *et al.* offers a distinctive perspective[87]. Although it does not involve conventional "N–N coupling" (as the product contains no N–N bond), its reaction strategy of "electrochemical surface generation of NH_4^+ and solution-phase pairing with NO_3^- to form an ionic nitrogen fertilizer" is structurally analogous to the Type III paradigm of "electrochemical intermediate generation and solution-phase bond formation". Specifically, NO_3^-/NO_2^- is reduced to NH_4^+ on the Ru_9Co_{91} surface (surface step); NH_4^+ then desorbs into the solution and combines with NO_3^- (either originally present or newly generated in the solution) via ionic bonding to form NH_4NO_3 (solution step). Although the "bond" formed in this system is ionic rather than covalent, its step sequence of "surface generation → desorption → solution encounter → bond formation"[87] is similar to the core strategy of Type III as defined in this Review. Another important contribution of this work is its demonstration that the solution-phase bond-forming step can proceed without any organic solvent or chemical mediator: because the step uses water as the sole medium and is driven by the stabilization from ionic bond formation, continuous production becomes feasible. This concept offers valuable insight for addressing the challenges of N–N coupling, where the instability of intermediates often necessitates reliance on organic solvents or mediators: if the coupling product itself possesses sufficient stability in solution (e.g., the ion-pair structure of hydrazinium salts)[88], it may substantially simplify the solution-phase design of Type III strategies, bringing them closer to practical implementation.

Jia *et al.* recently reported a cascade conversion from NO_x to N_2H_4: electrocatalytic reduction of NO_x to NH_3, followed by diphenyl ketone (DPK)-mediated and WO_3-catalyzed coupling, achieving an overall selectivity of 88.7%[89]. This strategy decouples electrocatalytic ammonia production from chemical coupling in both time and space: DPK condenses with NH_3 to form an imine intermediate ($Ph_2C{=}N^-$), whose steric hindrance and conjugation effects synergistically suppress over-reduction and hydrolysis; acetonitrile as a solvent extends the lifetime of the imine via hydrogen-bonding interactions; lattice oxygen on the WO_3 surface participates in dehydrogenation, driving the coupling of two imine units ($2\ Ph_2C{=}N^- \rightarrow Ph_2C{=}N{-}N{=}CPh_2$) with concomitant regeneration of DPK.

As illustrated in Figure 5, this work demonstrates a three-stage tandem paradigm involving electrochemical generation of inorganic intermediates, molecular engineering of organic mediators, and heterogeneous catalytic coupling. This strategy transfers the challenge of N–N bond-formation selectivity from surface electrocatalysis to tunable solution-phase organic chemistry, thereby providing a versatile platform for the synthesis of hydrazones, oximes, and N–N-containing heterocycles from NO_x.

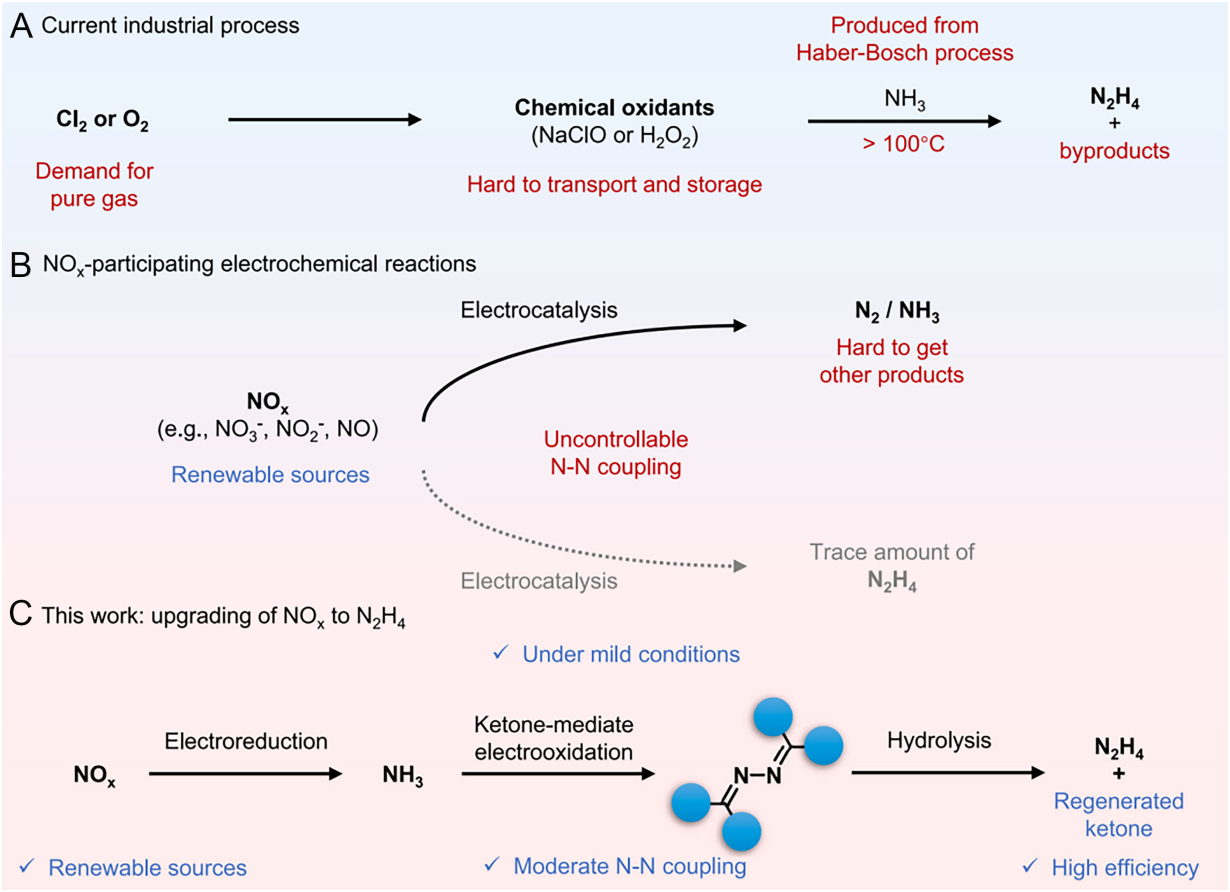

Figure 5. Schematic overview of the diphenyl-ketone-mediated cascaded pathway for hydrazine synthesis. Reproduced without modification from reference[89] under a CC BY-NC-ND 4.0 license.

S–N COUPLING: THEORETICAL FEASIBILITY AND CATALYST DESIGN PERSPECTIVES

Application value of target products

The sulfonamide moiety (–SO_2–NH–) is a privileged scaffold in medicinal chemistry, deeply embedded in numerous clinically approved drugs, including sulfa antibiotics, CO_{X-2} selective inhibitors, carbonic anhydrase inhibitor diuretics, and sulfonylurea hypoglycemic agents[90]. Their reduced derivatives, sulfinamides and sulfonylhydrazides, serve as versatile synthetic building blocks for constructing sulfur-nitrogen bonds and also exhibit notable biological activities such as protease inhibition and antitumor effects.

Type I: surface S–N coupling - formidable challenges

Within the Type I surface-direct-coupling framework, S–N bond formation requires co-adsorption of sulfur species and nitrogen intermediates (e.g., *NH_2) followed by lateral diffusion and coupling. This pathway is obstructed by the strong, irreversible chemisorption of sulfur species on most metal surfaces; these species can readily form dense sulfide layers that poison active sites, thereby suppressing the adsorption and activation of nitrogen intermediates from the outset. Realizing this pathway requires control of the co-adsorption of S, N, and H species, yet H, as a competitively dominant species, narrows the operating window amidst this three-way competition, and experimental examples remain scarce. Current efforts are largely confined to theoretical design explorations. One strategy employs transition metal sulfides (e.g., MoS_2, CoS_x) as platforms[91], leveraging their intrinsic sulfur-containing structure to provide inherent sulfur tolerance, while introducing independent nitrogen-reduction active centers via sulfur vacancies, metal doping, or

heterointerfaces. Ideally, sulfur species would be localized to the basal plane or sulfur edges, while nitrogen intermediates reside at metal edges or vacancies to achieve spatially proximate coupling[91]. However, theoretical simulations continue to reveal severe challenges: sulfur species preferentially occupy coordinatively unsaturated active sites, making it difficult to eliminate poisoning competition; moreover, the relatively low electrical conductivity and limited intrinsic nitrogen reduction activity of sulfides further restrict the accessible potential and current windows. These factors indicate that achieving simultaneous sulfur adsorption, nitrogen activation, and bond formation on a single surface is exceptionally difficult. Shifting the sulfur source from the surface to the solution phase via Types II and III represents a more viable alternative[92].

The above-mentioned sulfur-poisoning risk arises primarily in metallic catalyst systems. Non-metallic platforms (e.g., heteroatom-doped carbon, covalent organic frameworks) exhibit intrinsically weaker chemisorption of sulfur-related species and are less susceptible to irreversible sulfur-site passivation, making them theoretically promising candidates for revisiting Type I surface S–N coupling[13].

However, a new trade-off emerges for these non-metallic materials: their weak sulfur affinity is usually accompanied by insufficient adsorption strength toward critical nitrogen intermediates (*NH_2, *NHOH). Realizing Type I coupling demands balanced co-adsorption of both sulfur-containing reactants and reactive nitrogen intermediates on the same surface site, a benchmark not yet achieved experimentally for electrocatalytic nitrate- or N_2-reduction-driven S–N bond construction. Accordingly, non-metallic catalysts open up a prospective research direction for Type I S–N coupling, but substantial material optimization is still required before this pathway can become practically feasible.

Type II: surface-solution interfacial coupling - a promising route

The Type II strategy for S–N coupling achieves spatial separation by shifting the sulfur source from the surface to the solution phase: the electrode surface is responsible solely for generating and maintaining nitrogen-containing active intermediates (e.g., *NH_2 or near-surface enriched NH_2OH), while the sulfur source, present as dissolved species in the electrical double layer or near-surface solution, encounters the nitrogen intermediates at the interface for bond formation[93]. This design circumvents the competition between sulfur and nitrogen for adsorption sites, allowing already-optimized nitrogen reduction catalysts (such as Cu-based materials) to be used without the need to provide sulfur-activation functionality. Inorganic sulfur sources such as SO_2/SO_3^{2-} offer high atom economy when reacting with NH_2/NH_2OH[94], but require precise buffering of interfacial pH to maintain the nucleophilic activity of HSO_3^- while suppressing disproportionation. Organic thiols, although providing structural diversity, face strong competition from S–S oxidative coupling and cumulative sulfur poisoning of the cathode surface during prolonged electrolysis[58]. Dynamic potential operation strategies offer theoretical promise but lack experimental validation: pulsed electrolysis, by alternating between working and cleaning potentials, periodically removes adsorbed sulfur and modulates interfacial species concentrations, thereby suppressing homogeneous S–S coupling; flow electrolysis cells, in turn, leverage continuous flow to remove S–N products in a timely manner, reducing the near-surface concentration and residence time of sulfur species and mitigating poisoning. Combined with intrinsically sulfur-tolerant catalyst design (e.g., oxophilic surfaces or self-cleaning sulfur vacancies), Type II interfacial S–N coupling could provide a route to electrochemical sulfonamide production, bridging surface inorganic nitrogen reduction and organosulfur chemistry.

Type III: solution-phase S–N coupling—drawing on N–N tandem strategies

The Type III decoupling strategy can be extended to the S–N system: the electrode serves merely as a generator of NH_3 or NH_2OH, while solution-phase chemical catalysis forms the S–N bond. The ketone-mediated strategy may be adapted to this system: the ketone captures NH_3 to form an imine, which

subsequently undergoes nucleophilic addition-rearrangement with SO_2/SO_3^{2-} or thiols to construct sulfonamide scaffolds. This pathway circumvents the cumulative sulfur poisoning at the electrode surface and can fully leverage mature S–N bond-forming methodologies from organic synthesis. However, S–N and N–N couplings differ fundamentally in that the electrophilicity of SO_2/SO_3^{2-} is distinct from that of nitrous acid, and the nucleophilic attack of NH_3 on SO_2 is more strongly regulated by pH and solvation effects.

It is worth emphasizing an important thermodynamic pitfall for this solution-phase route: direct mixing of aqueous SO_2/SO_3^{2-} and electrogenerated NH_3 predominantly produces sulfamate adducts featuring S–O–N linkages, instead of the target sulfonamide with direct covalent S–N bonds, as S–O–N species are thermodynamically favored under aqueous conditions[95]. Several prospective chemical strategies can circumvent this unfavorable thermodynamic preference in future Type III S–N coupling studies. First, pre-activated sulfur electrophiles such as sulfonyl fluorides, sulfinyl chlorides or 1,4-diazabicyclo[2.2.2]octane-1,4-diium-1,4-disulfinate (DABSO) can replace free SO_2/SO_3^{2-}; these S(IV)/S(VI) reagents intrinsically favor nucleophilic substitution to form S–N bonds instead of S–O–N adducts. Second, instead of fully reduced NH_3, electrogenerated transient nitrogen intermediates (e.g., hydroxylamine, imines formed *in situ*) can serve as nitrogen-containing coupling partners, whose modified nucleophilic character disfavors sulfamate formation. Third, solvent-medium engineering by adopting mixed organic-aqueous or aprotic media suppresses hydration-promoted S–O–N formation and rebalances the relative thermodynamic stability between S–N and S–O–N products. Fourth, post-electrolysis homogeneous mediators or redox-catalytic steps can be introduced in a tandem fashion, potentially rearranging initially-formed S–O–N adducts toward desired S–N-containing scaffolds. Nevertheless, complete experimental realization combining electrocatalytic nitrate/N_2 reduction with these chemical strategies for sulfonamide synthesis has not yet been reported, and these strategies serve as guiding perspectives for further exploration. The independent optimization afforded by Type III renders it the most flexible and expandable pathway for exploring S–N electrocatalytic synthesis.

FROM CATALYST SITE DESIGN TO REACTION SYSTEM ENGINEERING

Core methodology: design principles for dual-region synergy

The shift from "ammonia production" to cross-phase N–N/S–N coupling examined in this Review highlights a key point: coupling reactions cannot be understood from isolated catalyst sites alone because bond formation may involve both surface and solution processes. Conventional ammonia-producing catalysis compresses all steps onto the surface, whereas coupling catalysis may extend the reaction space to the electrical double layer and even the bulk solution.

The catalyst is therefore a key component of a complete reaction system. Solvation effects, pH-controlled nucleophilicity/electrophilicity, the electron-shuttle function of redox mediators, and reactor configuration control of mass transport and residence time are all as important as the catalyst itself. The design target should therefore include the whole reaction system, guided by the following decision strategy: Regional Priority Principle: Determine the optimal reaction zone based on the chemical nature of the coupling system (poisoning propensity, solubility, thermodynamic stability). If intermediates can be co-adsorbed without poisoning, prioritize Type I (surface coupling), focusing on *H suppression and enhanced $*NH_2$ surface coverage. If coverage mismatch or mild poisoning exists, consider Type II (interfacial coupling), coordinating surface potential and solution pH to stabilize the intermediate oxidation state. If intermediates are highly unstable or the catalyst suffers severe poisoning, efforts should pivot to Type III (solution-phase tandem coupling), simplifying the electrocatalytic task to "high-yield generation of readily desorbable precursors" and leaving bond formation entirely to solution chemistry.

Decoupling for Efficiency Principle: When the surface environment (strongly reducing potentials, competitive adsorption) is unfavorable for bond formation, physical or chemical decoupling (e.g., tandem reactors, temporal separation via pulsed electrolysis) is often more effective than materials modification alone. In such cases, the catalyst's objective is no longer "to accomplish the entire reaction" but rather "to precisely generate and controllably release specific intermediates".

Priority order and roadmap of feasible pathways

Based on the above principles and the existing literature, we categorize the coupling pathways into three tiers according to experimental feasibility and theoretical maturity:

Near-term breakthrough: Type III solution-phase tandem coupling (electrochemical-chemical tandem)

Type III solution-phase tandem coupling is currently the only strategy to achieve clear proof of concept. The ketone-mediated N_2H_4 synthesis reported by Han and co-workers (88.7% selectivity) demonstrates the advantages of complete decoupling. The anode-cathode cascade electrolyzer developed by Loh and co-workers achieved a pyruvic oxime production rate of 2.61 $mmol \cdot cm^{-2} \cdot h^{-1}$ with an FE of 101% at 2.8 V; techno-economic analysis (TEA) identified flow rate as the most critical parameter (sensitivity: 0.912)[96]. Together, these two routes reveal that the principal advantage of Type III lies in engineering control of intermediate transport and reaction matching.

Mid-term development: Type II interfacial coupling (nitrate-derived nitrogen intermediates toward azo compounds)

This pathway is proposed based on established strategies for controlling nitrate-reduction intermediates and electrochemical N–N coupling. The core concept is to selectively arrest nitrate reduction at the NO_2^- or NO stage and promote subsequent encounters between these nitrogen intermediates and aromatic amine coupling partners in the near-electrode region. The current challenge is to establish a kinetic "nitrosation window" in which productive interfacial coupling can compete with deep hydrogenation and intermediate loss. Based on existing knowledge of nitrate-reduction selectivity, pulsed electrolysis, and interfacial regulation[56,79,80,84], we suggest prioritizing Cu-based catalysts, dynamic potential operation, and interfacial pH control for proof-of-concept studies. Direct nitrate-derived azo electrosynthesis remains a prospective target rather than an experimentally established pathway.

Long-term theoretical exploration: S–N coupling - theoretical projection and catalyst pre-design

To the best of our knowledge, direct electrosynthesis of sulfonamides using nitrate as the nitrogen source has not yet been demonstrated. One major challenge, particularly for conventional metallic catalysts, is the strong adsorption and accumulation of sulfur-containing species, which can interfere with nitrogen activation and catalyst stability[57]. Based on the analysis in this Review, we propose the following theoretical roadmap: deprioritize Type I surface coupling on conventional metallic catalysts, as the co-adsorption of sulfur and nitrogen is thermodynamically and kinetically nearly incompatible; Type II interfacial coupling deserves cautious exploration because spatial separation of nitrogen activation and the sulfur-containing coupling partner may reduce direct competition for surface sites. Sulfide-derived interfaces and sulfur-vacancy engineering offer potentially useful materials-design concepts[91], while pulsed electrolysis can dynamically regulate surface coverage and mitigate sulfur accumulation[57]. At the reactor level, flow configurations could also be explored to regulate near-electrode residence time, reactant supply, and product removal. These individual elements provide a basis for future Type II S–N studies, although their integration into nitrate-derived sulfonamide electrosynthesis remains to be experimentally demonstrated. A further priority is Type III (solution-phase tandem coupling), which remains the most modular long-term option because electrochemical generation of nitrogen-containing intermediates can be separated from downstream

sulfur chemistry. In this configuration, nitrate/N_2 electroreduction would first generate a sufficiently stable nitrogen-containing intermediate, whereas S–N bond formation would be independently optimized in a subsequent solution-phase step. Existing electrochemical S–N chemistry and SO_2-based organic synthesis provide relevant chemical precedents[92,95], although suitable sulfur electrophiles, mediators, and reaction conditions compatible with nitrate-derived intermediates remain to be identified.

Beyond these direct chemical considerations, cross-disciplinary studies in electrochemical and functional-material systems provide transferable design principles for the reaction-system engineering proposed here. Hollow and multi-shelled architectures demonstrate how spatial confinement, facilitated mass transport, and temporally programmed release can be integrated within a single material platform[97,98]. Studies of electrochemical energy-storage interfaces further illustrate the importance of defect and interface engineering[99], pore-size-dependent electric-double-layer regulation[100], and interfacial solvation, ionic flux, and electric-field control[101]. These concepts are particularly relevant to the present emphasis on matching intermediate generation, transport, and residence time across surface and solution regions. More directly, multicomponent electrocatalytic coupling studies highlight the need to integrate active-site coordination, interfacial mass transport, and reactor-level engineering[102]. Structural regulation of sulfur-containing materials[103], dynamic surface and interfacial control through pulsed electrochemistry[104], and mesostructure/composition regulation for selective electrosynthesis[105] further illustrate general strategies for controlling reaction kinetics and selectivity. At the device level, (bi)carbonate electrolysis emphasizes the importance of electrode, membrane, and flow optimization[106]. Finally, studies correlating crystallographic orientation and microstructure with transport properties, together with advanced electron-microscopy approaches for resolving structure-property relationships, provide broader methodological inspiration for catalyst microstructure design and characterization[107,108]. These cross-disciplinary examples are not cited as direct demonstrations of N–N or S–N coupling; rather, they illustrate transferable principles of confinement, interfacial regulation, transport engineering, structural control, and multiscale characterization that underpin the system-level framework proposed in this Review.

Reactor configuration constitutes another essential dimension for system-level optimization of N–N and S–N coupling. Distinct hardware setups are better matched to different coupling pathways. Conventional H-type electrolytic cells are well-suited for fundamental mechanistic research of Type I surface coupling, providing well-controlled static environments to probe intrinsic surface reaction kinetics. For Type II interfacial coupling with high mass-transport requirements, flow electrolyzers are preferred because they continuously refresh near-electrode reactant supply and remove accumulated by-products from the interfacial diffusion layer[109]. For Type III solution-phase tandem coupling, cascaded electrochemical–chemical reactor architectures are recommended, where the electrochemical intermediate-generation compartment and downstream homogeneous bond-formation unit are spatially separated[96].

Key operational parameters, including electrolyte flow rate and reactant concentration, strongly modulate coupling selectivity. Under low flow-rate conditions, intermediate residence time in the near-surface region is prolonged, which can favor interfacial Type II coupling; excessive flow rate, by contrast, sweeps reactive intermediates away from the electrode interface and suppresses interfacial bond-forming events. Reactant concentration also has competing effects: moderately elevated reactant concentration can boost intermediate population for coupling, yet excessively high concentration may trigger competing side reactions or accelerate poisoning phenomena, especially for S–N coupling scenarios. Appropriate operating windows must be optimized on a case-by-case basis according to the target coupling pathway.

Practical perspectives: catalyst deactivation, economic feasibility and reporting-metric standardization

Catalyst deactivation represents a practical barrier for scaling N–N and especially S–N coupling electrocatalysis. Four major deactivation modes deserve attention: (i) irreversible chemisorption of sulfur species and site poisoning, which is the dominant failure mode for metal electrodes used in S–N coupling; (ii) surface fouling by strongly adsorbed organic/nitrogen-containing intermediates or by-products accumulated during long-term electrolysis; (iii) potential-driven catalyst reconstruction, phase transformation, or element leaching under reductive cathodic conditions; (iv) gradual degradation of electrode-support interfaces under continuous operation[58]. These degradation mechanisms vary across three coupling pathways: Type I and Type II systems suffer more from surface poisoning and intermediate fouling, while Type III tandem setups shift major stability burdens toward the downstream homogeneous chemical unit rather than the electrocatalyst itself.

Regarding economic feasibility, current N–N/S–N coupling investigations are still limited to lab-scale proof-of-concept demonstrations, and comprehensive quantitative TEA is not yet feasible. Several core cost-related factors nevertheless deserve attention for future practical translation, including overpotential-associated energy input, feedstock price, catalyst material cost and service lifetime, as well as high costs of product separation and purification for target nitrogen-containing products from complex electrolyte mixtures. Advancing scalable catalyst manufacturing beyond small-batch laboratory synthesis is also a prerequisite for real-world deployment. Continuous-flow slurry electrolysis provides a promising high-throughput route to fabricate size-tunable electrocatalysts for electrochemical coupling applications[110]. In addition, inconsistent performance-reporting metrics hinder objective comparison across Type I, Type II, and Type III coupling pathways. Researchers should explicitly clarify whether reaction rates and Faradaic efficiencies are normalized against geometric electrode area or electrochemically active surface area (ECSA). Geometric-area normalization reflects device-level performance for practical cell evaluation; ECSA-normalized values are more suitable for intrinsic catalyst-activity comparison. Where mass-transport limitations are significant, mass-transport correction is strongly recommended to eliminate diffusion-induced performance bias. Together with stable-isotope verification and unified production-rate units, these normalization practices would substantially improve comparability among different coupling studies.

Moreover, considerable inconsistency persists across the literature regarding product-quantification workflows and performance-reporting units for N–N and S–N coupling systems. Colorimetric assays, nuclear magnetic resonance (NMR) spectroscopy, and chromatographic methods are all used for product detection, while production-rate units vary from mass-based to mole-based units, hindering direct comparison across studies[21]. To improve the reliability and comparability of product identification, two reporting practices deserve particular attention. First, researchers are strongly encouraged to use stable-isotope tracing when nitrate or N_2 is proposed as the nitrogen source. Wherever feasible, ^{15}N-labelled feedstocks should be used to verify isotope incorporation into the final coupling product, rather than only into intermediate nitrogen species. Established protocols for electrocatalytic synthesis from inorganic nitrogen sources demonstrate the utility of ^{15}N-labelled products and standardized product-validation procedures[21]. Second, researchers are encouraged to adopt unified molar-basis production-rate units (e.g., $\mu mol \cdot h^{-1} \cdot cm^{-2}$) for reporting coupling-product formation rates, facilitating more direct comparison among Type I, Type II, and Type III pathways.

CONCLUSION AND OUTLOOK

The core arguments of this Review can be distilled into three main points: First, breakthroughs in coupling catalysis require moving beyond the exclusive focus on "surface catalysis". Regarding the electrode surface as the sole arena for all transformations, this focus, while effective in conventional ammonia-production studies, may limit coupling reactions by overlooking the roles of the interfacial and solution regions in

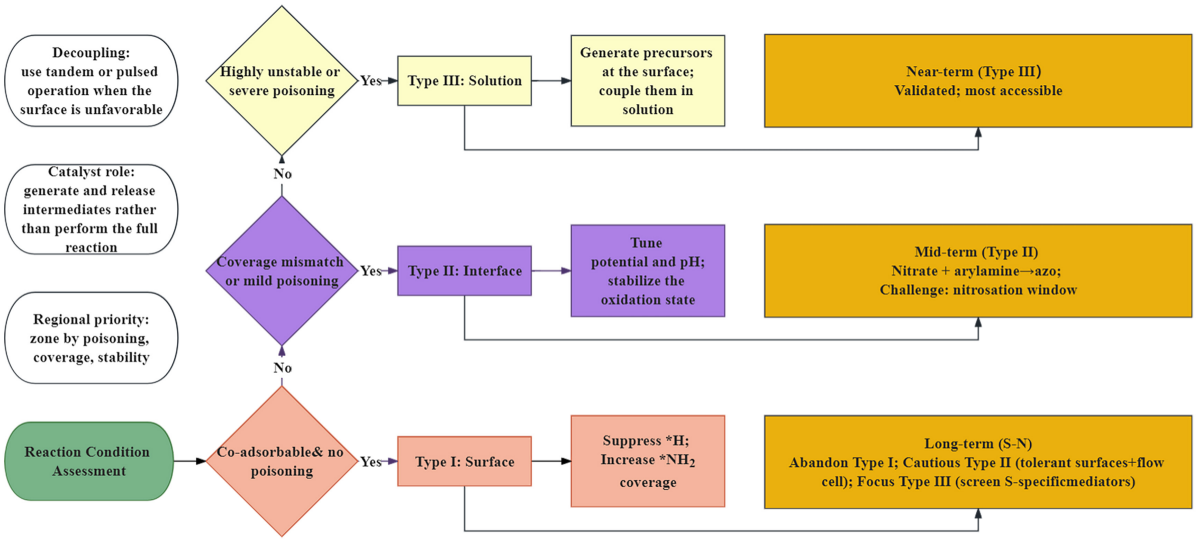

Figure 6. Decision-tree-based roadmap for selecting appropriate Type I/Type II/Type III coupling pathways for electrocatalytic N–N and S–N bond construction.

regulating substrate availability, intermediate transport, poisoning competition, and downstream bond-forming chemistry.

Second, the electrochemical-chemical tandem strategy is currently the best-established experimental option. Its modular nature makes it a promising platform for converting inorganic nitrogen sources into more complex products. Interfacial coupling may be useful in specific systems (e.g., azo synthesis), whereas surface-localized S–N coupling remains particularly challenging. Third, catalyst design needs to be redefined.

The catalyst should efficiently generate specific intermediates and release them controllably into solution. This objective focuses catalyst design on adsorption, activation, and selective partial reduction, while solution chemistry controls the subsequent bond-forming step. The division of functions should be determined according to the stability and reactivity of the relevant intermediates, as summarized in Figure 6.

Beyond these chemistry-specific conclusions, related fields of electrochemistry and functional materials provide transferable concepts for future reaction-system engineering. Data-driven electrolyte/interface analysis[111], interfacial thermodynamic and kinetic regulation[112], pulsed electrochemistry[104], hollow-structure confinement[113], suppression of competing hydrogen evolution[114], multiphysics system design[115], selectivity-oriented electrosynthesis[105], and externally assisted transport control[116] collectively offer broader inspiration for regulating reaction microenvironments, transport, and selectivity. These studies are cited as cross-disciplinary design precedents rather than direct demonstrations of N–N or S–N coupling.

DECLARATIONS

Authors' contributions

Completed the main writing of the manuscript: Hu, Y.; Wang, J. (Junxiao Wang)
Collected and integrated the relevant references: Wang, Z.; Wang, J. (Jiangyan Wang)
Designed the manuscript outline, offered professional guidance, and revised the initial draft: Wan, J.; Wang, D.

Availability of data and materials

Not applicable.

AI and AI-assisted tools statement

During the preparation of this manuscript, the AI tools DeepSeek (version 3.2, released 2025-12-01) and ChatGPT (OpenAI, version GPT5.6-Sol, released 2026-07-09) were used for language editing and editorial assistance. The tools did not influence the study design, data collection, analysis, interpretation, or the scientific content of the work. All authors take full responsibility for the accuracy, integrity, and final content of the manuscript.

Financial support and sponsorship

This work was supported by the National Key R&D Program of China (No. 2024YFA1509400), the National Natural Science Foundation of China (Nos. 22293043, 92572205, 22505267, 52272097), Shenzhen University 2035 Program for Excellent Research (No. 2024B005), Beijing Natural Science Foundation (No. 2242019) and IPE Project for Frontier Basic Research, China (No. QYJC-2023-08). Wang, D. acknowledges financial support from the Outstanding Scientific and Technological Innovation Talents Training Fund in Shenzhen.

Conflicts of interest

All authors declared that there are no conflicts of interest.

Ethical approval and consent to participate

Not applicable.

Consent for publication

Not applicable.

REFERENCES

1. Li, Q.; Li, Y.; Xu, B.; Yang, J.; Wang, Y. Gram-scale ammonia synthesis via electrochemical nitrate reduction using enzyme-inspired dual-atomic Cu catalyst. *Angew. Chem. Int. Ed. Engl.* **2025**, *64*, e202510139. DOI PubMed
2. Li, Z.; Shi, Z.; Ou, Y.; et al. Pulsed electrocatalysis driven efficient ammonia synthesis by facilitating *NOOH formation and balancing *H supply. *Angew. Chem. Int. Ed. Engl.* **2025**, *64*, e202510287. DOI PubMed
3. Sun, H.; Xia, Z.; Qi, Y.; et al. Tandem Cu-Co sites in MOF-818 for efficient ammonia electrosynthesis from nitrate in neutral media. *ACS. Catal.* **2025**, *15*, 16581-90. DOI
4. Wang, Y.; Hao, F.; Xu, H.; et al. Interfacial water structure modulation on unconventional phase non-precious metal alloy nanostructures for efficient nitrate electroreduction to ammonia in neutral media. *Angew. Chem. Int. Ed. Engl.* **2025**, *64*, e202508617. DOI PubMed
5. Gu, X.; Zhang, J.; Guo, S.; et al. Tiara Ni clusters for electrocatalytic nitrate reduction to ammonia with 97% faradaic efficiency. *J. Am. Chem. Soc.* **2025**, *147*, 22785-95. DOI PubMed PMC
6. Zhao, H.; Liu, P.; Cheng, X.; et al. A Cu-Cu_2O/Ni_2P heterostructure for efficient tandem catalysis of electrosynthesis of ammonia from nitrate reduction reaction in neutral medium. *Adv. Funct. Mater.* **2025**, *35*, 2425459. DOI
7. Ji, X.; Hu, R.; Li, J.; et al. Multiply nano-twinned copper as a “dual-site cooperative” catalyst for enhanced electrocatalytic nitrate reduction to ammonia. *Adv. Mater.* **2026**, *38*, e16937. DOI PubMed
8. Chang, H. M.; Fan, C.; Baltrusaitis, J.; Kim, H.; Pan, S. Y. Advancing twin transition in wastewater management for nitrogen cycle. *Water. Res.* **2026**, *300*, 125948. DOI PubMed
9. Chen, J. G.; Crooks, R. M.; Seefeldt, L. C.; et al. Beyond fossil fuel-driven nitrogen transformations. *Science* **2018**, *360*, eaar6611. DOI PubMed PMC
10. Su, Y.; Li, S.; Wang, X. Z.; et al. Application of high-entropy materials in promoting electrocatalytic nitrogen cycle. *Small. Methods.* **2025**, *9*, e01303. DOI PubMed
11. Feng, Y.; Ren, J. T.; Sun, M. L.; Yuan, Z. Y. Valorization systems based on electrocatalytic nitrate/nitrite conversion for energy supply and valuable product synthesis. *Chem. Sci.* **2025**, *16*, 1528-59. DOI PubMed PMC
12. Zhang, T.; Che, Z.; Song, Y.; et al. Breaking the performance limit of pure metals for N_2 electroreduction. *Angew. Chem. Int. Ed. Engl.* **2025**, *64*, e202514028. DOI PubMed
13. Chen, Z.; Liu, G.; Zhao, Y.; et al. Co_1 Zn single-atom alloy boosts active hydrogen spillover for highly efficient electrosynthesis of ammonia over 2 A cm^{-2} current density. *Angew. Chem. Int. Ed. Engl.* **2026**, *65*, e23740. DOI PubMed

14. Jiang, H.; Chen, G. F.; Savateev, O.; et al. Enabled efficient ammonia synthesis and energy supply in a zinc-nitrate battery system by separating nitrate reduction process into two stages. *Angew. Chem. Int. Ed. Engl.* **2023**, *62*, e202218717. DOI PubMed
15. Rao, F.; Xiao, Q.; Wei, Y.; Wang, J.; Yu, R.; Wang, D. Balanced polysulfide containment and lithium ion transport in lithium-sulfur batteries via nitrogen-doped carbon hollow multi-shelled structures on modified separators. *Chem. Res. Chin. Univ.* **2024**, *40*, 690-8. DOI
16. Wang, H.; Gong, G.; Sun, G.; Qi, J.; Yu, R.; Wang, D. Regulating oxygen vacancy defects in heterogeneous NiO-$CeO_{2-\delta}$ hollow multi-shelled structure for boosting oxygen evolution reaction. *Chem. Res. Chin. Univ.* **2024**, *40*, 475-83. DOI
17. Wang, H.; Wei, P.; Wang, J.; Wang, D. Hollow multishelled structure reviving lithium metal anode for high-energy-density batteries. *Chem. Res. Chin. Univ.* **2024**, *40*, 428-36. DOI
18. Su, F.; Wan, J.; Wang, D. Hollow multi-shelled structure photoelectric materials: multiple shells bring novel properties. *Chem. Res. Chin. Univ.* **2024**, *40*, 413-27. DOI
19. Li, A.; Liu, M.; Wu, H.; et al. One-pot electrochemical synthesis of (hydroxyamino)methanesulfonate from CO_2, nitrate/nitrite, and sulfite. *J. Am. Chem. Soc.* **2026**, *148*, 22532-40. DOI
20. Zhang, C.; Liu, J.; Cao, Q.; et al. O_2-mediated synergistic oxidation of aqueous bisulfite and nitrite: a key pathway for sulfate and nitrate formation in atmospheric sulfur-nitrogen cycles. *Environ. Sci. Technol.* **2026**, *60*, 10950-60. DOI
21. Wu, Y.; Liu, X.; Huang, Y.; Meng, N.; Zhang, B. Electrocatalytic C–N bond construction from inorganic nitrogen sources in water. *Nat. Protoc.* **2026**, *21*, 3098-126. DOI PubMed
22. Liu, Z.; Ma, G.; Li, J.; et al. Directing the electrochemical C–N coupling toward efficient amide synthesis via ammonia activation-mediated pathway. *Angew. Chem. Int. Ed. Engl.* **2025**, *64*, e202518108. DOI PubMed
23. Qian, Q.; Liu, Q.; Wang, M.; et al. Dual-site cooperation for synergistic optimization of the band structure and spin state to facilitate C–N coupling reaction. *Proc. Natl. Acad. Sci. U. S. A.* **2025**, *122*, e2508077122. DOI PubMed PMC
24. Zhang, L. H.; Zhou, J.; Zhan, J.; Zhu, X.; Li, F.; Yu, F. Enhanced CO_2 activation through spin states engineering boosting urea electrosynthesis from Co-reduction of CO_2 and NO_2^-. *Angew. Chem. Int. Ed. Engl.* **2026**, *65*, e6197518. DOI PubMed
25. Wang, R.; Liu, Y.; Kong, Y.; Chen, Q.; Zhao, S. Boosting synergistic catalysis C–N coupling via stabilizing close zn/ti bimetallic sites for electrocatalytic urea synthesis from CO_2 and nitrite. *ACS. Catal.* **2025**, *15*, 2703-14. DOI
26. Wang, Z.; Chen, M.; Lu, G.; et al. Single-atom catalysts toward electrocatalytic urea synthesis*via* C–N coupling reactions. *Chem. Commun.* **2025**, *61*, 13601-15. DOI PubMed
27. Yuan, Y.; Kou, M.; Zhao, J.; Zhao, J.; Yang, X. Regioselective electrocatalytic urea synthesis via spin-polarized PdCu/TiO_{2-x} with oxygen vacancy engineering. *Carbon. Hydrogen.* **2025**, *27*, 344-53. DOI
28. Wu, X.; Chen, Y.; Tang, B.; et al. CeO_x-integrated dual site enhanced urea electrosynthesis from nitrate and carbon dioxide. *Nat. Commun.* **2025**, *16*, 8785. DOI PubMed PMC
29. Liu, Y. Y. Fabrication of Mo-based electrocatalysts and their performance in ammonia synthesis. Ph.D. Dissertation, University of Science and Technology of China, Hefei, 2021. DOI
30. Xu, L.; Yao, Y.; Wu, W.; et al. Electrochemistry-mediated synthesis of hydrazine from ammonia. *Angew. Chem. Int. Ed. Engl.* **2026**, *65*, e20218. DOI PubMed
31. Wang, F.; Gerken, J. B.; Bates, D. M.; Kim, Y. J.; Stahl, S. S. Electrochemical strategy for hydrazine synthesis: development and overpotential analysis of methods for oxidative N–N coupling of an ammonia surrogate. *J. Am. Chem. Soc.* **2020**, *142*, 12349-56. DOI PubMed PMC
32. Zhong, Q.; Jung, J.; Kohrs, D.; et al. Deciphering the mechanism of on-surface dehydrogenative C–C coupling reactions. *J. Am. Chem. Soc.* **2024**, *146*, 1849-59. DOI PubMed
33. Liu, H.; Jia, S.; Wu, L.; et al. Circumventing scaling relations via gradient orbital coupling promotes ammonia electrosynthesis on cobalt catalyst. *Angew. Chem. Int. Ed. Engl.* **2025**, *64*, e202510478. DOI PubMed
34. Zhao, Y.; Li, Q. Q.; He, Q. F.; et al. *In Situ* raman spectroscopy reveals the multifunctional role of interfacial water in CO_2-to-C_2 electroreduction on Cu(*hkl*) surfaces. *J. Am. Chem. Soc.* **2025**, *147*, 30230-8. DOI PubMed
35. Zhang, C.; Zhang, J.; Jiao, Z.; Lum, Y.; Wang, Z. Tuning eley-rideal mechanism in electrochemical acetylene semi-hydrogenation. *Angew. Chem. Int. Ed. Engl.* **2025**, *64*, e202512218. DOI PubMed PMC
36. Guo, C.; Yang, R.; Meng, N.; et al. Nitrate-stabilized $Cu^{\delta+}$ sites promote selective CO_2 electroreduction to ethanol for tandem acetamide electrosynthesis. *Angew. Chem. Int. Ed. Engl.* **2026**, *65*, e5526884. DOI PubMed PMC
37. Huang, X.; Xie, S.; Li, Y.; et al. Controlled interruption of electrochemical nitrite reduction for switchable NH_2 OH and formamide synthesis. *Angew. Chem. Int. Ed. Engl.* **2026**, *65*, e5328209. DOI PubMed

38. Hu, Q.; Peng, O.; Liu, J.; et al. Coupling nitrate electrochemical reduction and nitrite oxidation of ethanol for acetamide synthesis. *Nat. Commun.* **2025**, *17*, 1340. DOI PubMed PMC
39. Shi, Y.; Yang, D. Enantioselective reductive couplings and related transformations under cooperative photoredox catalysis. *Chem. Soc. Rev.* **2026**, *55*, 2441-64. DOI PubMed
40. Gu, L.; Song, N.; Wu, Z.; Luo, H.; Chen, J.; Yang, J. Regulation of active hydrogen and nitrate concentration: pulsed potential strategies in nitrate electroreduction microenvironments. *Angew. Chem. Int. Ed. Engl.* **2026**, *65*, e25547. DOI PubMed
41. Fan, Y.; Yan, Y.; Nwokonkwo, O.; et al. Tuning nitrate reduction reaction selectivity via selective adsorption in electrified membranes. *Nat. Chem. Eng.* **2025**, *2*, 379-90. DOI
42. Lei, B.; Li, B.; Wang, Y.; et al. Managing active hydrogen species on ternary copper-based catalyst for efficient electrochemical ammonia synthesis from nitrate. *J. Am. Chem. Soc.* **2026**, *148*, 13774-84. DOI PubMed
43. Zheng, L.; Zhang, Y.; Chen, W.; et al. Carbon-extraction-triggered phase engineering of rhodium nanomaterials for efficient electrocatalytic nitrate reduction reaction. *Angew. Chem. Int. Ed. Engl.* **2025**, *64*, e202500985. DOI PubMed
44. Guo, H.; Zhang, X.; Lyu, J.; et al. Constructing asymmetrically coordinated transition metal single atoms with high loadings for ammonia electrosynthesis. *Nat. Synth.* **2026**. DOI
45. Jia, S.; Wang, R.; Li, W.; et al. Interfacial water frustration for nitrate semireduction to hydroxylamine at industrial-relevant currents. *J. Am. Chem. Soc.* **2025**, *147*, 47848-58. DOI PubMed
46. Han, T.; Wei, L.; Lv, L.; et al. Spin effect of transition metal oxides on ammonia decomposition. *J. Am. Chem. Soc.* **2026**, *148*, 14426-34. DOI PubMed
47. Xu, H.; Peng, J.; Li, P.; et al. Gradient adsorption energy strategy unlocks ultra-long stability and efficient electrocatalytic ammonia synthesis from nitrate over CoP/Cu_3P. *Angew. Chem. Int. Ed. Engl.* **2026**, *65*, e22410. DOI PubMed
48. Zhao, T.; Chen, Y.; Wang, K.; Ho, S. H. Neutral-pH electrocatalysis for nitrate reduction to ammonia: toward sustainable nitrogen management in aquatic systems. *Environ. Sci. Technol.* **2026**, *60*, 7605-27. DOI PubMed
49. Wen, W.; Fang, S.; Zhou, Y.; Zhao, Y.; Li, P.; Yu, X. Y. Modulating the electrolyte microenvironment in electrical double layer for boosting electrocatalytic nitrate reduction to ammonia. *Angew. Chem. Int. Ed. Engl.* **2024**, *63*, e202408382. DOI PubMed
50. Xue, X.; Chen, A.; Liu, J.; et al. Suppression of ammonia slip by smart reductants in selective catalytic reduction of nitrogen oxides. *Angew. Chem. Int. Ed. Engl.* **2026**, *65*, e8855639. DOI PubMed PMC
51. Wu, B.; Li, X.; Hou, T.; et al. Oxygen-bridged Cu and V dual metal sites for enhanced photo-oxidative coupling of benzylamine. *J. Am. Chem. Soc.* **2025**, *147*, 46997-7007. DOI PubMed
52. Guo, C.; Shen, L.; Tang, Y.; et al. Ru single atoms anchored on Co-NC for nitrate electroreduction toward NH_3 synthesis. *Nano. Res.* **2025**, *18*, 94907623. DOI
53. Yang, C.; Tian, S.; Liu, R.; et al. Nanoconfinement-driven electronic structure and local microenvironment modulation for electrochemical nitrate reduction to ammonia synthesis. *Coord. Chem. Rev.* **2026**, *562*, 217940. DOI
54. Tang, Y.; Li, J.; Li, Y.; et al. Langmuir-hinshelwood pathway enables 1000-h stable nitrate-to-ammonia electroreduction at 1 A cm^{-2}. *Nat. Commun.* **2026**, *17*, 7326. DOI PubMed PMC
55. Zhao, H.; Wang, D.; Liu, N.; et al. Dynamic proton allocation drives high-efficiency nitrate electroreduction on high-entropy alloy aerogels across broad concentration ranges. *Angew. Chem. Int. Ed. Engl.* **2026**, *65*, e20035. DOI PubMed
56. Torabi, K.; Liu, R.; Troglauer, D. L.; et al. Reductive nitrogen species activation via pulsed electrolysis: recent advances and future prospects. *Angew. Chem. Int. Ed. Engl.* **2025**, *64*, e202516909. DOI PubMed PMC
57. Hou, Z.; Ma, Y.; Wu, Y.; Cao, W.; Guo, Z.; Wang, C. Pulsed electrolysis prevents sulfur poisoning for sustained sulfide valorization. *Adv. Mater.* **2026**, *38*, e73096. DOI PubMed PMC
58. Yu, J.; Zhang, G.; Zeng, Y.; et al. Selective electrochemical C–N coupling via synergetic chemical and electrochemical microenvironment regulation strategies. *J. Am. Chem. Soc.* **2025**, *147*, 43594-603. DOI PubMed
59. He, Y.; Mo, S.; Zeng, X.; et al. Paired electrolysis enables selective C–N coupling for the synthesis of nitrogenous aromatics. *Nat. Synth.* **2026**, *5*, 1416-27. DOI
60. Ni, J.; Wei, J.; Yu, Y.; et al. Revealing the role of interfacial water in pH-dependent hydroxylamine electrosynthesis over Bi-based catalysts. *ACS. Catal.* **2025**, *15*, 15153-61. DOI
61. Huang, S.; Zhi, Y.; Wang, Z.; et al. Redox-mediated electrified method for green and low-cost spent lithium-ion battery materials recycling. *ChemRxiv.* **2026**. DOI
62. Zhang, X.; Zhang, Y.; Li, M.; et al. Screening and dissecting electroorganic synthesis by mass spectrometry decoupling of electrode and homogeneous processes. *Nat. Commun.* **2025**, *16*, 7452. DOI
63. Yang, M.; Wang, W.; Zhao, Z.; et al. Boosting nitrate reduction through Ru-CO_3^{2-} microenvironment modulated hydrogen-bond networks. *Angew. Chem. Int. Ed. Engl.* **2026**, *65*, e21249. DOI PubMed

64. Zhang, H.; Raciti, D.; Hall, A. S. Chaotropic anions promote electrochemical C–C Bond formation by reshaping interfacial solvation. *J. Am. Chem. Soc.* **2026**, *148*, 14904-11. DOI PubMed
65. Wang, T.; Iriawan, H.; Peng, J.; et al. Confined water for catalysis: thermodynamic properties and reaction kinetics. *Chem. Rev.* **2025**, *125*, 1420-67. DOI PubMed
66. Du, J.; Wu, Y.; Fang, S.; et al. Nano-confinement engineering boosts C–N coupling for urea electrosynthesis. *Nat. Commun.* **2025**, *17*, 1008. DOI PubMed PMC
67. Blum, S. P.; Karakaya, T.; Schollmeyer, D.; Klapars, A.; Waldvogel, S. R. Metal-free electrochemical synthesis of sulfonamides directly from (hetero)arenes, SO_2, and amines. *Angew. Chem. Int. Ed. Engl.* **2021**, *60*, 5056-62. DOI PubMed PMC
68. Yang, Z.; Gao, R. T.; Wu, L.; Wang, L. Ultralow-potential photoelectrochemical synthesis of hydroxylamine and oximes. *Angew. Chem. Int. Ed. Engl.* **2026**, *65*, e25106. DOI PubMed
69. Zhang, H.; Raciti, D.; Hall, A. S. Disordered interfacial H_2O promotes electrochemical C–C coupling. *Nature. Chem.* **2025**, *17*, 1161-8. DOI PubMed
70. Long, J.; Hu, C.; Yao, Q.; et al. Light-promoted hydrazine dehydrogenation over Ni/NH_2-MIL-125: unraveling mechanisms for efficient hydrogen production. *Adv. Sci.* **2026**, *13*, e19320. DOI PubMed PMC
71. Kumari, S.; Carmona, A. V.; Tiwari, A. K.; Trippier, P. C. Amide bond bioisosteres: strategies, synthesis, and successes. *J. Med. Chem.* **2020**, *63*, 12290-358. DOI PubMed PMC
72. Saha, P.; Amanullah, S.; Dey, A. Electrocatalytic reduction of nitrogen to hydrazine using a trinuclear nickel complex. *J. Am. Chem. Soc.* **2020**, *142*, 17312-7. DOI PubMed
73. Kundu, J.; Bhoyar, T.; Park, S.; Jin, H.; Lee, K.; Choi, S. I. Recent advances in single- and dual-atom catalysts for efficient nitrogen electro-reduction and their perspectives. *Adv. Powder. Mater.* **2025**, *4*, 100279. DOI
74. Xing, C.; Wang, X.; Zhou, H.; Sun, Y.; Guan, X. Sulfate radical promotes aminyl radical coupling for selective ammonia conversion to harmless dinitrogen. *Water. Res.* **2026**, *295*, 125576. DOI PubMed
75. Zhang, W.; Yao, Y.; Hu, Y.; et al. Bypassing hydrogenation pathway for sustainable nitrate water remediation via direct N–N coupling. *Angew. Chem. Int. Ed. Engl.* **2026**, *65*, e7025421. DOI PubMed
76. Li, W. Q.; Chen, Y.; Lu, X.; et al. Photoinduced nitrogen spillover enables ammonia synthesis on iron-aluminium dual-site catalysts. *Nat. Synth.* **2026**, *5*, 1008-20. DOI
77. Tahir, W.; Wei, Y.; Wang, M.; et al. Covalent organic frameworks on Cu_2O nanocubes as rapid proton/electron transfer gates for efficient NH_3 electrosynthesis from nitrate in neutral media. *J. Am. Chem. Soc.* **2026**, *148*, 743-55. DOI
78. Bhowmick, S.; Adalder, A.; Maiti, A.; et al. Controlling electrocatalytic nitrate reduction efficiency by utilizing dπ-pπ interactions in parallel stacking molecular systems. *Chem. Sci.* **2025**, *16*, 4806-14. DOI PubMed PMC
79. Wu, K.; Wu, W.; Liu, S.; et al. Switching N-N versus N-H couplings in nitrate electroreduction with CuPd surface atomic motifs. *Angew. Chem. Int. Ed. Engl.* **2026**, *65*, e24218. DOI PubMed
80. Zhou, N.; Wang, Z.; Zhang, N.; Bao, D.; Zhong, H.; Zhang, X. Potential-induced synthesis and structural identification of oxide-derived cu electrocatalysts for selective nitrate reduction to ammonia. *ACS. Catal.* **2023**, *13*, 7529-37. DOI
81. Fang, L.; Wang, S.; Song, C.; Yang, X.; Li, Y.; Liu, H. Enhanced nitrate reduction reaction via efficient intermediate nitrite conversion on tunable Cu_xNi_y/NC electrocatalysts. *J. Hazard. Mater.* **2022**, *421*, 126628. DOI PubMed
82. Filippi, M.; Ju, W.; Möller, T.; Liang, L.; Wang, X.; Strasser, P. Tandem architectures for electrochemical CO_2 reduction: from coupled atomic sites to tandem electrolysers. *Nat. Nanotechnol.* **2026**, *21*, 494-507. DOI PubMed
83. Tan, Y.; Fu, J.; Luo, T.; Liu, K.; Liu, M. Theoretical insights into the selectivity of single-atom Fe–N–C catalysts for electrochemical NO_x reduction. *J. Am. Chem. Soc.* **2025**, *147*, 4937-44. DOI PubMed
84. Qiao, W.; Waseem, I.; Shang, G.; et al. Paired electrochemical N–N coupling employing a surface-hydroxylated Ni_3Fe-MOF-OH bifunctional electrocatalyst with enhanced adsorption of nitroarenes and anilines. *ACS. Catal.* **2021**, *11*, 13510-8. DOI
85. Liu, H.; Bai, L.; Bergmann, A.; Cuenya, B. R.; Luo, J. Electrocatalytic reduction of nitrogen oxide species to ammonia. *Chem* **2024**, *10*, 2963-86. DOI
86. Sun, Q.; Xue, Y.; Niu, H.; et al. Sustainable synthesis of ammonium nitrate from air and water via tandem plasma-electrolyzer system. *Angew. Chem. Int. Ed. Engl.* **2026**, *65*, e3006166. DOI PubMed PMC
87. Han, S.; Yang, K.; Gao, L.; et al. Synthesis of liquid nitrogenous fertilizer via a nitrogen conversion balance. *Nat. Sustain.* **2025**, *8*, 1068-76. DOI
88. Robinson, R. J.; Mccrone, W. C. Crystallographic data 169. Hydrazine nitrate (l). *Anal. Chem.* **1958**, *30*, 1014-5. DOI
89. Jia, S.; Zhang, L.; Liu, H.; et al. Upgrading of nitrate to hydrazine through cascading electrocatalytic ammonia production with controllable N-N coupling. *Nat. Commun.* **2024**, *15*, 8567. DOI PubMed PMC

90. Kokre, S. J.; Kavalapure, R. S.; Huddi, S. S.; et al. Sulfonamides: a versatile scaffold for diverse biological activity. *Results. Chem.* **2025**, *18*, 102858. DOI
91. Wang, T.; Guo, Z.; Oka, H.; Kumatani, A.; Liu, C.; Li, H. Origin of electrocatalytic nitrogen reduction activity over transition metal disulfides: critical role of *in situ* generation of S vacancy. *J. Mater. Chem. A.* **2024**, *12*, 8438-46. DOI
92. Liu, G.; Chen, Y.; Chen, Y.; et al. Indirect electrocatalysis S–N/S–S bond construction by robust polyoxometalate based foams. *Adv. Mater.* **2023**, *35*, 2304716. DOI PubMed
93. Xu, Y.; Zhu, C.; Luo, J.; Zhang, L. Electrocatalytic C(sp^3)–H/S–H coupling: accessing thioethers via a stabilized electrophile. *CCS. Chem.* **2026**, 1-12. DOI
94. Qiu, G.; Zhou, K.; Gao, L.; Wu, J. Insertion of sulfur dioxide via a radical process: an efficient route to sulfonyl compounds. *Org. Chem. Front.* **2018**, *5*, 691-705. DOI
95. Vogel, P.; Turks, M.; Bouchez, L.; Marković, D.; Varela-Álvarez, A.; Sordo, J. A. New organic chemistry of sulfur dioxide. *Acc. Chem. Res.* **2007**, *40*, 931-42. DOI PubMed
96. Peng, O.; Hu, Q.; Jin, M.; et al. Hydroxyl and nitrate co-upgrading to oxime via anode-cathode cascade electrolyzer. *Nat. Commun.* **2025**, *16*, 6145. DOI PubMed PMC
97. Hou, P.; Yang, N.; Wang, D. Multi-functional hollow structures for intelligent drug delivery. *Chem. Res. Chin. Univ.* **2024**, *40*, 394-412. DOI
98. Mao, D.; Wang, C.; Li, W.; et al. Hollow multishelled structure: synthesis chemistry and application. *Chem. Res. Chin. Univ.* **2024**, *40*, 346-93. DOI
99. Wang, B.; Chen, X.; Chen, X.; et al. High-performance MnO_2-based cathodes for aqueous zinc-ion batteries: challenges, strategies, and perspectives. *eScience. Energy.* **2025**, *1*, 100008. DOI
100. Lee, E.; Lee, J.; Kang, D. H.; et al. Electrowetting-driven capacitance enhancement dependent on charge carrier and nanopore size. *eScience. Energy.* **2025**, *1*, 100006. DOI
101. Yang, G.; Zhang, X.; Zhang, H.; et al. Hydrogen bond-anchored interfacial engineering for stable and high-performance aqueous zinc-ion batteries. *eScience. Energy.* **2026**, *2*, 100027. DOI
102. Zhao, Y.; Mei, X.; Han, C.; Xu, W. Multicomponent electrocatalytic coupling of CO_2 with small molecules: from active-site coordination to reactor-level integration. *eScience. Energy.* **2026**, *2*, 100064. DOI
103. Wang, Y.; Zhou, Z.; Li, B.; Yu, C.; Du, Z.; Ai, W. Lattice-strain-engineered FeS_2/rGO composite for ultrafast and durable sodium-ion batteries. *eScience. Energy.* **2026**, *2*, 100074. DOI
104. Chen, W.; He, Y.; Zou, Y.; Wang, S. Pulsed electrochemistry: a pathway to enhanced electrocatalysis and sustainable electrosynthesis. *Natl. Sci. Open.* **2024**, *3*, 20240047. DOI
105. Gai, T.; Ai, Y.; Li, W. Rare-earth-metal-alloyed mesoporous PtPb nanosheets for selective electrosynthesis of glyceric acid from glycerol upcycling. *Natl. Sci. Open.* **2025**, *4*, 20250042. DOI
106. Xing, K.; Chen, J.; Li, Y. Towards energy-efficient (bi)carbonate electrolysis: Innovation and challenges. *Natl. Sci. Open.* **2024**, 20240039. DOI
107. Qu, Y.; Zhao, B.; Zhao, W.; Deng, Y. Achieving superior thermoelectric transport in bismuth antimony telluride thin films via orientation and microstructure regulation. *Natl. Sci. Open.* **2025**, *4*, 20250008. DOI
108. Nan, P.; Ge, B. Electron microscopy approaches to thermoelectrics: recent advances and emerging opportunities. *Natl. Sci. Open.* **2025**, *4*, 20250006. DOI
109. Chen, Z.; Zhang, L.; Sun, S.; Zhang, G. Electrochemical cell designs for efficient carbon dioxide reduction and water electrolysis: status and perspectives. *Adv. Mater.* **2025**, *37*, 2505287. DOI PubMed PMC
110. Xiong, J.; Lian, G.; Li, K.; et al. Electrifying catalyst production by continuous-flow slurry electrolysis. *JACS. Au.* **2025**, *5*, 5427-37. DOI PubMed PMC
111. Chen, Y.; Liu, Y.; He, Z.; et al. Artificial intelligence for the understanding of electrolyte chemistry and electrode interface in lithium battery. *Natl. Sci. Open.* **2024**, 20230039. DOI
112. Wang, Z.; Chen, J.; Yang, Z.; et al. Zinc utilization rate in aqueous batteries: regulation of interfacial thermodynamics and kinetics. *Natl. Sci. Open.* **2025**, *4*, 20250044. DOI
113. Son, Y.; Kim, D.; Kim, J.; Jin, H.; Kwon, T.; Lee, K. Hollow nanostructures with controlled internal voids: Beyond simple surface area maximization of the electrocatalyst. *Natl. Sci. Open.* **2026**, *5*, 20260012. DOI
114. Liu, Y.; Wu, Z.; Qin, Z.; Liu, Y.; Hu, W. Recent progress in inhibition of hydrogen evolution reaction in alkaline Al-air batteries. *Natl. Sci. Open.* **2024**, *3*, 20240037. DOI
115. Feng, Y.; Zhang, Z.; Gong, L.; et al. Environmental multi-physics coupled tribovoltaic effect for energy harvesting. *Natl. Sci. Open.* **2025**, *4*, 20240032. DOI

116. Wang, Z.; Xia, J.; Garry, R.; Weitz, D. A.; Li, X. Recent progress on acoustofluidic manipulation of cells and particles. *Natl. Sci. Open.* **2025**, *4*, 20230080. DOI